Coastal Engineering 194 (2024) 104623

Contents lists available at ScienceDirect

Coastal Engineering

journal homepage: www.elsevier.com/locate/coastaleng

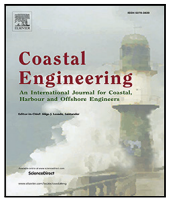

Prototype data analysis of the dynamics of the Venice gate-barriers during an extreme storm event

Paolo Sammarco [a], Piera Fischione [a,*], Alessandro Romano [b,c], Giorgio Bellotti [b], Sergio Dalla Villa [d]

[a] University of Rome Tor Vergata, Department of Civil and Computer Science Engineering, via del Politecnico 1, Rome, 00133, Italy
[b] Roma Tre University, Department of Civil, Computer Science and Aeronautical Technologies Engineering, Rome 00146, Italy
[c] IHCantabria - Instituto de Hidráulica Ambiental de la Universidad de Cantabria, Calle Isabel Torres 15, Santander 39011, Spain
[d] Consorzio Venezia Nuova, Arsenale Nord Castello 2737/f, Venezia 30122, Italy

ARTICLE INFO

Keywords:
MoSE system
Venice lagoon
Storm surge
Gates dynamics
EOF

ABSTRACT

The MoSE barriers system was designed and constructed at the inlets of the Venice Lagoon (Italy) in order to limit and tame the flooding events in the Lagoon areas and in the City. The success of the design and operation of the system has been demonstrated by the significant reduction in the number and intensity of floods in the lagoon since its beginning of operations in 2020. In this study, we investigate the dynamical behavior of the MoSE system at full-scale by analyzing the barriers behavior during the severe storm event of November 22nd, 2022. In particular, the dynamical response of the Chioggia barrier to waves and storm surge is studied in detail. Spectral analysis of field records, barrier and inlet modal analyses and Empirical Orthogonal Functions (EOF) techniques are applied to provide a key for interpreting the actual behavior of such a complex system during a storm event, highlighting dominant frequencies and checking for the occurrence of resonance phenomena. First, a brief review of the experimental and theoretical studies carried out over the past forty years is given. Modal patterns of gates oscillations detected via EOF analysis confirm the presence of the eigenmodes of both the barrier and the inlet; however, the gates oscillations during the considered event are mild and the hydraulic performances of the system are satisfactory for the severe event studied. Further field measurements and future severe events should be studied to reach extended conclusions.

1. Introduction

1.1. Context and motivation

During the last seven decades up to 2022 the city of Venice has faced an increasing number of flood events, the well-known phenomenon of "*acqua alta*", that impacted life style, economics and impaired the architectural and historical heritage of the City. This phenomenon is due to a combination of astronomical tides, storm surge, and seiches in the Adriatic Sea (Međugorac et al., 2018; Pasquali et al., 2019), exacerbated by a transient and now stabilized small subsidence in the north Adriatic Sea (Tosi et al., 2013). The complex flooding defense system of MoSE (Modulo Sperimentale Elettromeccanico) consists of four barriers, each made of a variable number of floating gates hinged along a common axis across the bottom of each Venice Lagoon inlet (Fig. 1). During a storm event the gates, which are otherwise laying horizontally on the seabed, are raised to a specific angle by pumping compressed air into the previously water-filled gates, so that the surge is kept outside the lagoon. The design and construction of the MoSE system took more than forty years since its ideation, but it has significantly contributed to the flooding safety of the Lagoon and the City since its beginning of operation in 2020.

The first raising of the gates in real necessity occurred in 2020; as of June 2024, the MoSE has been "called on duty" 84 times. The effectiveness of the MoSE system's design and construction is demonstrated by its successful operations and functioning, as well as by the significant reduction in the number and intensity of extreme flood events in the lagoon over the past four years (Alberti et al., 2023; Mel et al., 2023).

One concern during the design stage, besides the gates response in non-resonant conditions, has been the potential activation of synchronous or subharmonic resonance of spatially out-of-phase gates' motion (natural modes of the system) for a specific set of incident wave frequencies. This motivated extensive experimental campaigns and theoretical studies of the gates dynamics under waves action and a design of the gates geared to avoid such excitation phenomena (see Section 1.2).

* Corresponding author.
E-mail addresses: piera.fischione@uniroma2.eu, piera.fischione@uniroma2.it (P. Fischione).

https://doi.org/10.1016/j.coastaleng.2024.104623
Received 16 May 2024; Received in revised form 20 September 2024; Accepted 20 September 2024
Available online 26 September 2024

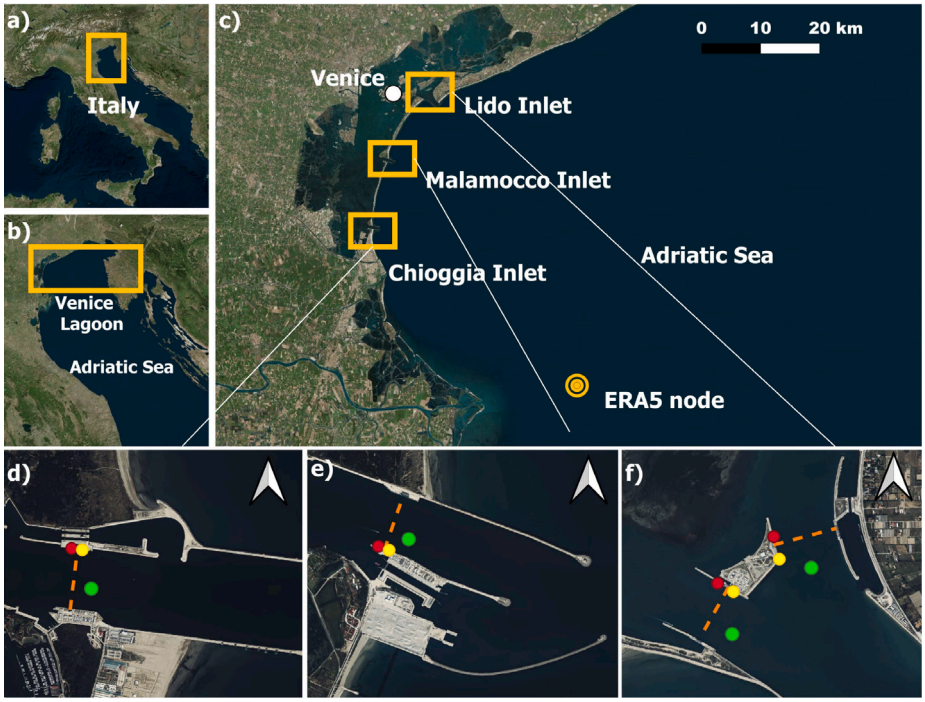

Fig. 1. Area of Interest. Panel (a) Overview of Italy and the area of interest (orange square). Panel (b) Zoomed-in view showing the northern Adriatic region, with the orange square indicating the specific area of interest of the Venice Lagoon. Panel (c) View of the Venice Lagoon. The orange rectangles highlight the inlets of the lagoon. The ERA5 node (45°N, 12.75°E) is represented by a thick orange circle. The white circle indicates the position of the city of Venice. Detailed views of the inlets of the lagoon are provided in panels: (d) Chioggia, (e) Malamocco, and (f) Lido. The southernmost inlet in panel (f) is Lido San Nicolò, while the northernmost is Lido Treporti. In panels (d), (e) and (f), the green circles represent the ADCPs positions, the red and yellow circles represent the radar sensors positions lagoon side and seaward respectively. The dark orange dashed lines represent the barriers.

In the present new era of Operations and Maintenance of the MoSE some questions still remain open. Were the natural modes' periods and patterns of the actual barriers (scale 1:1) properly predicted? Do these natural modes manifest themselves in a manner similar to that revealed by the experimental testing and the analytical theories? Can the barrier natural modes and the inlet modes be excited and to what extent do they affect gates response? Considered that in the first years of operation, no unpredicted response was ever observed and that oscillation amplitudes have always been below the envelope of predictions, what is the role played also by the feedback control system of the barriers? The analyses presented here contribute to answering these questions. One more question remains: do the actual ballast water, head difference (sea vs. lagoon), actual real sea state in front of the barrier, structural details of the gates, viscous dissipation and friction, all combine to alter the predicted periods of the natural modes and the likelihood of being excited? The answer to this question is object of ongoing research and not considered here.

1.2. Literature review

The idea and conceptualization of the MoSE system date back to the severe flooding event causing significant damage of November 4th 1966 (Trincardi et al., 2016). Since then, the entire spectrum of the fields of Coastal, Civil and Environmental Engineering has been challenged by this project, with contributions from a large number of national and international research institutions and laboratories (*Centro Sperimentale di Voltabarozzo, Delft Hydraulics Laboratories, Deltares, Estramed, Massachusetts Institute of Technology, Protecno, University of Padua*), design and construction firms, united to form the "Consorzio Venezia Nuova" (from now on CVN). One of the many significant challenges has been the modeling of the complex dynamic behavior of the floating gates in waves and currents. In this context, investigations were conducted by analytical, numerical and experimental means. Experimental model tests covered vertical and inclined gates in 2D wave flumes, in 3D wave tanks, and the whole four barriers and inlets in 3D layouts, with scales ranging from 1:64 to 1:10 (Consorzio-Venezia-Nuova, 1988, 2002a,b,c, 2003a,b). Gates were subjected to regular and irregular, linear and nonlinear waves, combined with currents. The extensive experimental campaigns highlighted the excitation of a subharmonic resonance phenomenon in which the gates oscillate at a frequency half of that of the incident waves and in opposition of phase with the immediate neighboring gates. Other spatial patterns and associated frequencies were also observed with the same excitation mechanism, suggesting the presence of more than one natural mode for a given set of gates.

In order to interpret and model this nonlinear phenomenon, analytical and numerical theories have been developed for vertical gates in equilevel and in an infinite channel with vertical walls by Mei et al. (1994) and Sammarco et al. (1997a,b), while Blondeaux et al. (1993a,b), Vittori et al. (1996) and Vittori (1997) analyzed the simplified geometry of a continuous vertical membrane. Mei et al. (1994) and Sammarco et al. (1997a,b) have explained the origin of the natural modes and the excitation mechanism, which are similar to the excitation of edge waves on a beach. The weakly nonlinear theory of Sammarco et al. (1997a,b) describes the amplitude of the modal oscillations as a function of the geometrical and inertial characteristics of the gates, the depth of the channel and the amplitude of the incident wave motion. They also showed that in the case of a modulated carrier incident wave, the gates response is at first modulated with the same frequency as the incident wave and then, for a higher modulational amplitude, becomes chaotic.

Liao and Mei (2000) extended the linear theory of Mei et al. (1994) and used the hybrid finite-element method to take into account the prototype geometry of the inclined gates and the lagoon-sea level difference for a two-gates system in a channel. The linear theory of Li and Mei (2003a) determined the $N-1$ eigenfrequencies of an array of N vertical gates in a channel and provided their $N-1$ values and the $N-1$ corresponding modal shapes as a function of the geometric and

inertial characteristics of the gates and of the channel depth. The theory also highlighted that the modal shapes are a discontinuous replication of a cosine function of gradually lower spatial frequency as the order increases from 1 to $N-1$.

According to the weakly nonlinear theory of Sammarco et al. (1997b), the subharmonic resonance of natural modes occurs for gates in an infinite or very long channel, where, at first order, there is no radiation of waves associated with modal gates' motion (perfectly trapped modes). Similarly to the excitation of edge waves on a beach, only a second order amplitude wave of twice the frequency of the trapped mode can excite the mode itself.

This resonance mechanism is less pronounced when considering the actual contours of the open lagoon and sea sides. In this case, wave/energy radiation associated with the natural modes is possible already at the leading order, so that the natural modes of the barriers can also be resonated synchronously.

Indeed, Adamo and Mei (2005) developed a linear theory for a vertical gates array forced by monochromatic incident waves, assuming that the lagoon side opens to a semi-infinite half-plane domain rather than a semi-infinite channel. This configuration allowed for radiation on the lagoon side at first order, so that trapping would no longer be perfect and therefore synchronous excitation be possible. Narrow frequency peaks were found at the same frequencies as in Li and Mei (2003a), with the spatial oscillation replicating the corresponding modal shapes. Synchronous and subharmonic resonance are therefore possible mechanisms of excitation of the natural modes of the barrier in the prototype case. Panizzo et al. (2006) analyzed the experimental data of the full 3D model (scale 1:60) of the Chioggia inlet and barrier via the Empirical Orthogonal Functions (EOF) method and showed that in storm condition the patterns and frequencies of a subset of the $N-1$ natural modes can be synchronously and subharmonically excited, together with the spatially in-phase motion.

During testing and design, concerns about the impact of model scale on nonlinear responses and natural periods measurements led to comparing physical models at scales 1:60, 1:30, and 1:10 (Consorzio-Venezia-Nuova, 2002c). The comparisons revealed no significant trends, with the value of the first natural period remaining consistent across all scales.

The three inlets of the Venice Lagoon (Lido, Malamocco and Chioggia) spanned by the four barriers (Lido Tre Porti and Lido San Nicolò, Malamocco and Chioggia respectively) are susceptible to long period oscillations due to excitation of their natural modes (see Adami et al., 1995). Indeed, when the gates are raised, these three inlets are closed on one end (barrier) and open to the Adriatic Sea. The low frequency band of the wave spectra penetrating the inlets encompasses the natural frequencies of the inlets and can directly excite these modes.

1.3. Aim of the study

The economical Benefits of the MoSE already surpassed the economical costs (Giupponi et al., 2024) when on November 22nd, 2022, the raising of the gates halted outside the lagoon the highest storm surge event since 1966, which would have otherwise caused substantial damages to the City. Indeed, the event of November 22nd, 2022 is the most severe that occurred since the beginning of operations both in terms of levels and wave height. In this work we investigate the dynamics of such a complex system, i.e. the inlets, the barriers, the lagoon, the water levels and the waves, during this event and also provide answers to the key questions still open.

1.4. Approach

The event is analyzed by means of spectral and Empirical Orthogonal Functions techniques applied to the field records of waves, water levels and gates oscillations time series. In order to provide a key for interpreting the behavior of the full-scale system, results are compared with the computed natural modes' eigenfrequencies and modal shapes of both the barrier and the inlet. The natural modes frequencies are calculated via the model of Li and Mei (2003b); the natural frequencies of the inlets are calculated using the technique of Bellotti (2020), Bellotti et al. (2012a,b) and Bellotti and Romano (2017). In the paper, these different techniques are combined and applied to the full-scale case, aimed at quantifying and analyzing the main phenomena that play a role in the dynamical response of the MoSE.

The dynamical behavior of the Chioggia inlet is analyzed in detail. This inlet has been chosen as a proof of concept for the application of the proposed approach, based on the application of different techniques, for the following reasons: (1) the orientation of the inlet makes it prone to wave penetration of waves coming from a wide range of direction (both *Scirocco* and *Bora*); (2) the barrier has been the most thoroughly investigated in previous studies (e.g. Consorzio-Venezia-Nuova, 2002c; Panizzo et al., 2006).

The paper is divided into five sections: Section 2 presents an overview of the gates system and a description of the general context and the facilities involved. Section 3 describes the metocean characteristics of the event of November 22nd, 2022, along with the gates angular position measured during the event. In Section 4 details of the analyses of the dynamic behavior of the gates at Chioggia inlet are given, while discussion is provided in Section 5.

2. The Venice Lagoon and the MoSE system

2.1. The Venice Lagoon

The Venice Lagoon is a tidal marsh area located along the Italian coasts of the northern Adriatic Sea (Fig. 1*a,b,c*). It covers an area of about 700 km^2, characterized by several small islands, tidal flats, and channels, reaching depths of about 20 m and surrounded by shallow waters of about 1 m depth (Fagherazzi et al., 1999; Carniello et al., 2005). The city of Venice stands out in the middle of the lagoon (Fig. 1*c*). The lagoon is separated from the Adriatic Sea by a coastal barrier that spans from Jesolo in the North to Chioggia in the South. The sea and the lagoon are connected by three inlets: Chioggia (Fig. 1*d*), Malamocco (Fig. 1*e*) and Lido (Fig. 1*f*), from South to North.

The main wind systems that characterize the Adriatic Sea, and consequently influence the levels in the lagoon, are regionally known as *Bora* and *Scirocco*. *Bora* is a cold and strong wind, which blows roughly parallel to the lagoon's major axis (NE direction). *Scirocco*, weaker than *Bora*, is a warmer wind that blows in South-East direction; due to its larger fetch (Fig. 1*b*) often causes high waves and water set-up in the northern part, enhanced by the semi-enclosed shape and shallow bathymetry of the Adriatic Sea. When *Scirocco* drops or switches to *Bora*, seiches can be generated (Lionello et al., 2021), lasting several days after the storm event ends. Thus, seiches on the Adriatic Sea have a different time scale from the local phenomena considered here, which instead are characterized by a time scale ranging from a few hours to tens of seconds.

The currents in the lagoon are mainly due to the astronomical tide (Gačić et al., 2004). The principal tidal components that play a significant role in the Adriatic Sea, and hence that influence the levels at the lagoon, are seven (among the others, see Defant, 1961; Gačić et al., 2004) with a mainly diurnal and semidiurnal microtidal regime.

2.2. The gates barriers

MoSE is a system consisting of four barriers, one at each inlet at Chioggia and Malamocco, and two barriers for the Lido inlet (the barriers of Lido San Nicolò and Lido Treporti). They are designed to disconnect temporarily the Venice Lagoon from the sea and protect the city in the event of significant storm surge (so called *acqua alta*). Each barrier is made of a (varying — see Table 1) number of gates, each about 20 m wide, hinged at the base along a common axis, able

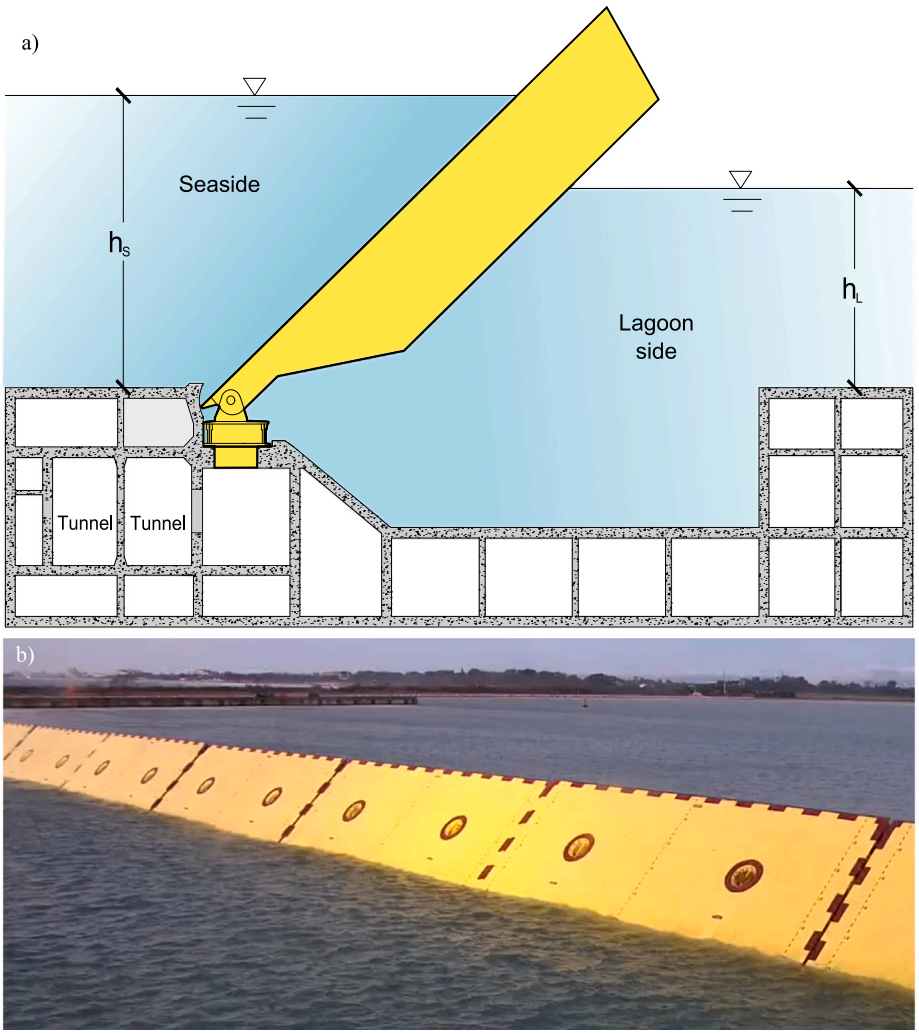

Fig. 2. Panel (a). Scheme of a single gate hinged at the cellular caisson that lies on the inlet bottom. h_S and h_L are the sea and lagoon levels, respectively. Panel (b). The MoSE barrier of Lido San Nicolò during the operation phase. The picture is taken from the seaside towards the lagoon side. Photo courtesy of Consorzio Venezia Nuova.

Table 1
Design characteristics of the barriers and the lagoon inlets.

Inlet	Channel depth (m)	Barrier length (m)	Gates number	Gate thickness (m)	Gate length (m)	Design angle (deg)
Lido Treporti	6	420	21	3.60	18.60	40.0
Lido San Nicolò	12	400	20	4.00	26.70	45.0
Malamocco	14	380	19	4.50	29.55	45.0
Chioggia	11	360	18	5.00	27.25	42.5

to rotate independently (Fig. 2, panel *a*). The gates are hidden in their housing, that consists of special concrete caissons that lie on the bottom of the channel and form the foundation of the barriers. Each caisson hosts three gates. Tunnel segments are part of the caissons that, once connected, form a continuous tunnel that allows technical inspections (Fig. 2, panel *a*). The equipment necessary for pumping the compressed air into the gates is installed in buildings located at the sides of each barrier. The caissons and the gates, in their rest position, do not protrude above the seabed, thus ensuring no disruption for local maritime traffic and flushing tidal currents.

The gates consist of steel box-like structures attached by two hinges to the caissons. Each gate has a width of 19.92 m and its design inclination angle and length are proportional to the depth of the inlet channel, so to ensure hydraulic disconnection between the sea and the lagoon when raised (Fig. 2, panel *b*). Table 1 summarizes the main characteristics of the barriers and of the channel inlets.

Each gate relies on the buoyancy mechanism to be raised. The barrier is raised only during storm surge events: compressed air is pumped in each gate, gradually causing a larger part of the water originally present inside the gate to be expelled and the gate structure to rotate around its axis, until an inclined equilibrium position is reached. Once the level surge retreats and the sea and lagoon reach acceptable levels, the air in the gates is released, water enters, and the gates return to their bottom rest position.

The raising of the gates is carried out according to a precise procedure. Generally, the gates are lifted in groups with a predefined order, but controlled independently of each other. The angle of inclination relative to the horizontal plane of each gate is measured using electronic inclinometers, installed within the gate and at each hinge, that measure the instantaneous inclination of the gate at a frequency of 1.0 Hz and with a tolerance of 0.2°.

The gates are raised when the predicted water level exceeds an alert level, that could lead to the flooding of the City. The alert level is

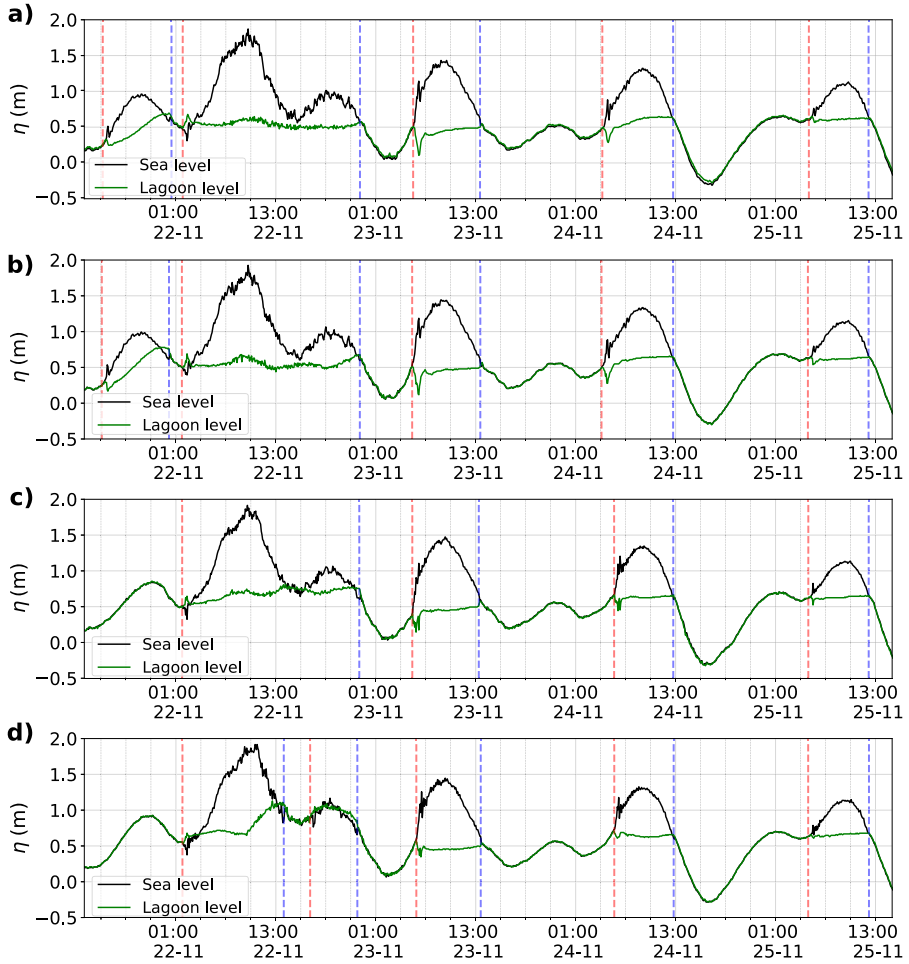

Fig. 3. Tidal levels recorded by the radar sensors at each inlet from November 22nd to 25th in ZPDS datum: *(a)* Lido Treporti; *(b)* Lido San Nicolò; *(c)* Malamocco; *(d)* Chioggia. The black line is for seaside levels and the green line is for lagoon side levels. The red dashed lines indicate the raising of the barrier and the blue lines the lowering.

+1.10 m measured with respect to the Punta della Salute datum (ZPDS), the local vertical reference system that differs from the Italian altimetric national datum (IGM) of about additional 0.235 m. Throughout the paper the IGM Italian national datum is used, except for Section 3.

Once all the gates have emerged and the inlet is closed, the inclinometers and the tracking system that modulates the air injection maintain the design angle in response to the head difference changes (feedback control system). The feedback control system is a Split Range Control Loop and operates at the time scale of seconds (Consorzio-Venezia-Nuova, 2009). The system introduces an additional source of damping, which is expected to have an influence in damping waves with wave period larger than 10 s.

3. The event of November 22nd, 2022

This section presents the description of the storm event of November 22nd, 2022, providing an overview of the hydraulic forcings (sea levels and waves) of the MoSE system. To this end, the hindcasted time series and measurements of water levels and waves (Section 3.1) and inclination angles of the gates (Section 3.2) are described in detail.

3.1. Characterization of the storm event

The following measurements provided by CVN at the three inlets are described: (i) sea levels measured both seaside and lagoonside (measurement locations are indicated by the yellow and red circles in Fig. 1, panels *d, e* and *f* respectively); (ii) waves measured by the Acoustic Doppler Current Profilers (ADCPs) located in front of each barrier, and reported as green circles in Fig. 1, panels *d, e* and *f*. Furthermore, offshore waves and winds have been extracted from the ERA5 hindcast dataset (Hersbach et al., 2020) at the point with coordinates 45.00°N, 12.75°E, identified by the orange circle in Fig. 1*c*.

A detailed description of the storm event is provided by Mel et al. (2023). They report that from the middle of November 2022, a large cyclonic system hit the north-western regions of Europe. On the days of 21st and 22nd November, the low-pressure area moved from the Ligurian Sea to the central part of Italy, reaching a minimum of almost 985 hPa. This system triggered intense *Scirocco* winds over the Adriatic Sea, that strengthened during the day 22nd and gradually shifted towards *Bora*. The combination of low pressure and winds forced a relevant storm surge in the Northern Adriatic Sea, that superposed on a spring tidal phase, resulting in a significant storm surge event. To protect the city of Venice from flooding, the MoSE system has been activated several times during those days.

Fig. 3 shows the water levels recorded by the radar sensors at each inlet, seaward (black lines) and lagoon side (green lines). In each panel, the red dashed lines indicate the time when the barriers were raised, while the blue dashed lines refer to the time of barriers lowering. On the 22nd, the absolute level peak occurred in the morning, at about 09:40 h at Lido and Malamocco and 10:30 h at Chioggia, followed by a minimum around 16:00 h and a new relative maximum around 19:00 h. The two peaks levels (seaside) on November 22nd are summarized in Table 2 and both are higher than the alert level of 1.10 m ZMPS. Therefore, the MoSE system has been activated, resulting in an extended closure of the inlets lasting 21 consecutive hours. Note that at the Chioggia inlet, located in the southern part of the lagoon, the

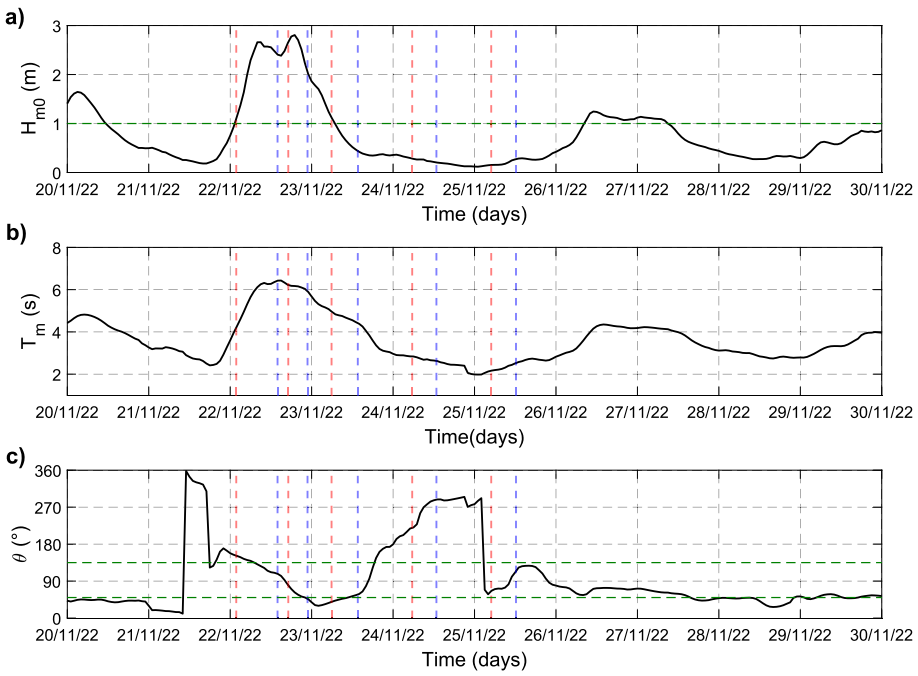

Fig. 4. Time series of H_{m0} (panel a), Tm (panel b), and mean direction (°N) (panel c) extracted from ERA5 in the time period ranging from November 20th, 2022, to November 30th, 2022. The dashed red and blue lines indicate the times of raising and lowering of the first gates of the Chioggia barrier, respectively.

Table 2
Maximum levels recorded at the lagoon inlets with respect to ZPDS datum (seaside).

Inlet	Peak 1		Peak 2	
	Hour	Level (m)	Hour	Level (m)
Lido Treporti	09:40	1.87	19:00	1.01
Lido San Nicolò	09:40	1.93	19:00	1.07
Malamocco	09:40	1.91	19:00	1.05
Chioggia	10:30	1.92	19:30	1.17

barrier was temporarily reopened during the event to lower the water levels (lagoon side) raised by the *Bora* wind blowing directly on the lagoon water surface. Specific protocols and criteria, not described in detail here, are adopted to manage the reopening procedures.

Fig. 3 shows the effectiveness of the MoSE system in protecting the lagoon from the storm surge. The black and green lines represent the recorded water levels at the seaside and lagoon side respectively. The water levels exhibit two main peaks during the 22nd November, one in the morning and the other in the afternoon (hereinafter Peak 1 and Peak 2, respectively). The maximum water levels during the day are summarized in Table 2. In fact, despite the very large surge recorded in front of the inlets, just behind the barriers the water levels remained well below the threshold that represents the level at which flooding of the Venice city would otherwise occur. During the event, the MoSE system has withheld a significant head difference between the lagoon and sea sides, that has reached the maximum values at 09:40 h of 1.27 m, 1.28 m, 1.20 m for respectively Treporti, San Nicolò and Malamocco; the maximum value recorded at Chioggia is 1.22 m (h 09:15). Mel et al. (2023) have shown that, without the MoSE system, the water levels in the Venice Lagoon would have been the highest ever recorded.

We now turn to the description of wave forcing.

Fig. 4 shows the ERA5 time series of offshore significant wave height H_{m0} (panel *a*), average wave period T_m (panel *b*), and mean wave direction θ (panel c) over the time interval ranging from November 20th to 30th, 2022. On day 22nd, the offshore significant wave height reached almost 3.0 m, with T_m around 6.5 s. The polar diagram in Fig. 5, shows the waves direction and height. In the early hours of

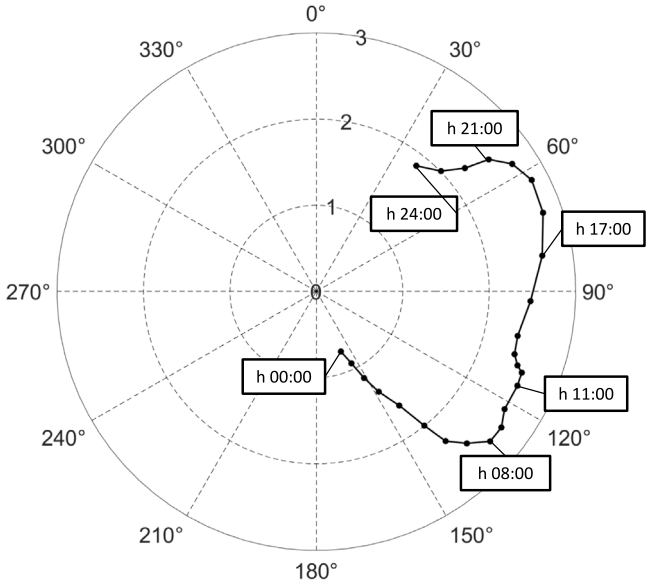

Fig. 5. Polar plot of the direction and H_{m0} at the ERA5 node during November 22nd, 2022. The black dots identify the hours of the day.

November 22nd the average wave direction was between 120°N and 170°N, i.e. *Scirocco*. At about 8:00 h, H_{m0} reached 2.8 m and the direction of approximately 130°N. These conditions are renowned to drive significant storm surge events (Orlić et al., 1994). Throughout the day, the offshore wave direction gradually rotated towards 60°N, i.e. *Bora*. Therefore, during the day, the offshore wave direction has aligned, at successive times, with the axis of the lagoon inlets, resulting in more pronounced wave penetration.

The time series of significant wave height measured by the ADCP in front of each barrier on November 22nd and averaged every 15 min, are reported in Fig. 6. The inlets of Lido and Malamocco, are more exposed to the waves from *Scirocco*: the wave height in these channels reaches a

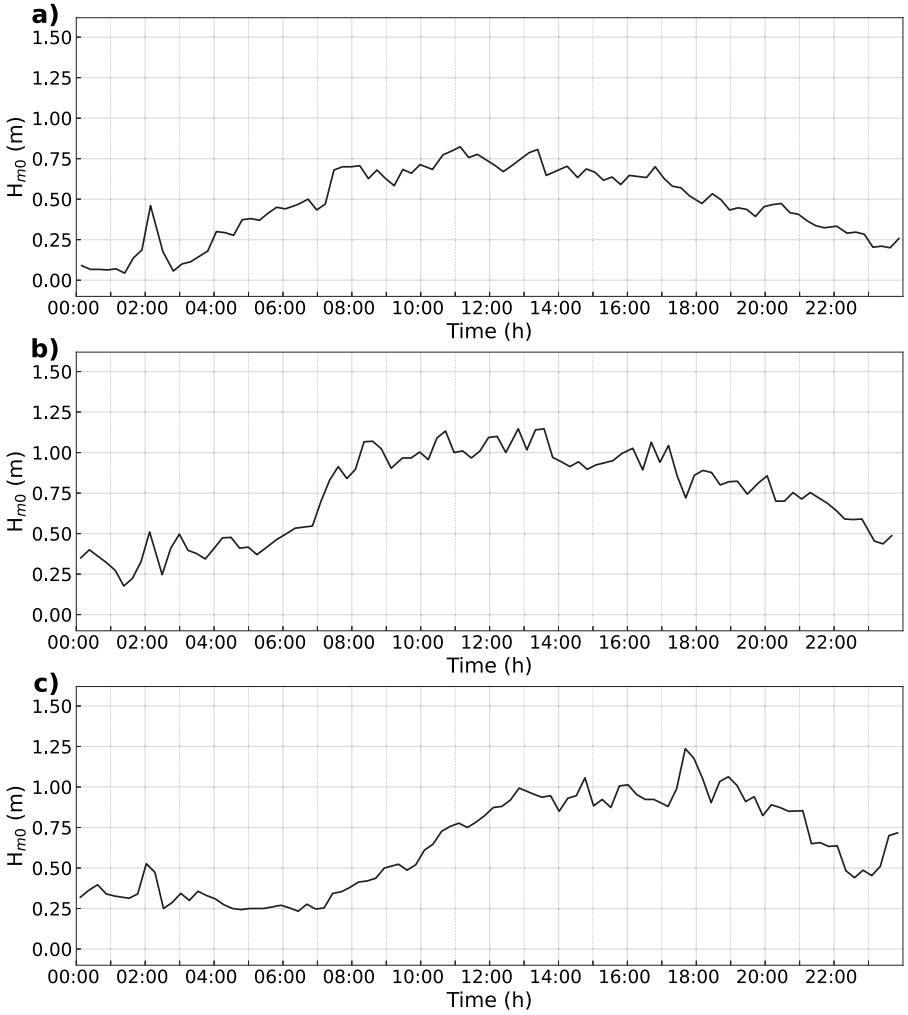

Fig. 6. H_{m0} time series at Lido San Nicolò inlet (panel a), Malamocco (panel b) and Chioggia (panel c).

maximum between 12:00 h and 14:00 h. Chioggia is more prone to the north-eastern *Bora* waves and, consequently, experiences the maximum wave height later, at about 18:00 h.

It is worth to notice that the wave fields at the positions of the ADCPs are the results of the superposition of the effects of many different physical phenomena. First, the waves that penetrate into the inlet, undergo diffraction at the mouth and reflection along the sides of the channel. In addition, reflection takes place at the barriers when they are closed. The oscillations of the gates, although small, are also a further source of radiating waves, that propagate back towards the sea. It is therefore difficult to associate the measurements with a progressive wave field.

Finally, the raising of the barriers induces translatory waves that appear in the wave height records as spurious sea states with larger significant wave height than expected, as for example in the time series at around 2:00 h (Fig. 6). The return period of the event of November 22nd, 2022, is estimated to be of the order of 30 years.

3.2. Processing of measured gates inclinations

In this subsection, the analysis of the gates inclination time series during the event of November 22nd, 2022 is considered. The dataset is represented, for each barrier, by the time series of the angles of the gates, namely $\theta_j(t_m)$. Here, j represents the gate ($j = 1, \ldots, N$, with N the number of gates in the barrier), while m represents the generic time level at which the angle was sampled, with $\Delta t = t_{m+1} - t_m = 1$ s the sampling interval. The recorded time series are analyzed and processed into statistical parameters, that requires calculation of average quantities. Specifically, the operator $\langle\cdot\rangle$ identifies averaging over the N gates of the considered barrier at a given time t_m, while $\overline{(\cdot)}^{\tau}$ indicates time average on a generic time window of duration $\tau = M\Delta t$ (in minutes), M being the number of samples. Hence, we first define the average angle of the gates barrier $\langle\theta\rangle(t_m)$. It is the spatial average of all the N gates inclination angles at each barrier at any given time t_m. The angle $\overline{\theta}_j^{\tau}$ is the time-averaged angle of the generic gate j over a window of duration $\tau = M\Delta t$ (in minutes). It is also possible to define the standard deviation σ_j^{τ} of the jth gate over the same interval τ (in minutes). The average angle of the barrier, averaged over the time interval τ, is $\overline{\langle\theta\rangle}^{\tau}$.

In Fig. 7, the time series $\langle\theta\rangle$ of the four barriers are shown. The considered time interval is the entire day of November 22nd. The barriers were raised at around 02:00 h. In about 1 h all the gates had been raised and the lagoon isolated from the sea. As previously mentioned, the Chioggia inlet was reopened during the event to lower the water levels raised by the *Bora* wind blowing on the lagoon. Thus, the operational intervals of the Chioggia barrier were from 2:00 h to 14:00 h and from 17:00 h to around 23:00 h. The figure shows that the average working angle of each barrier slightly changed during the day, according to the water level variations. In the first hours of the day, the gates experienced negligible oscillations, since short waves (see Fig. 6) were very mild in the inlets. On the contrary, starting at 07:00 h, the wave height increased and the average angle of the barriers showed

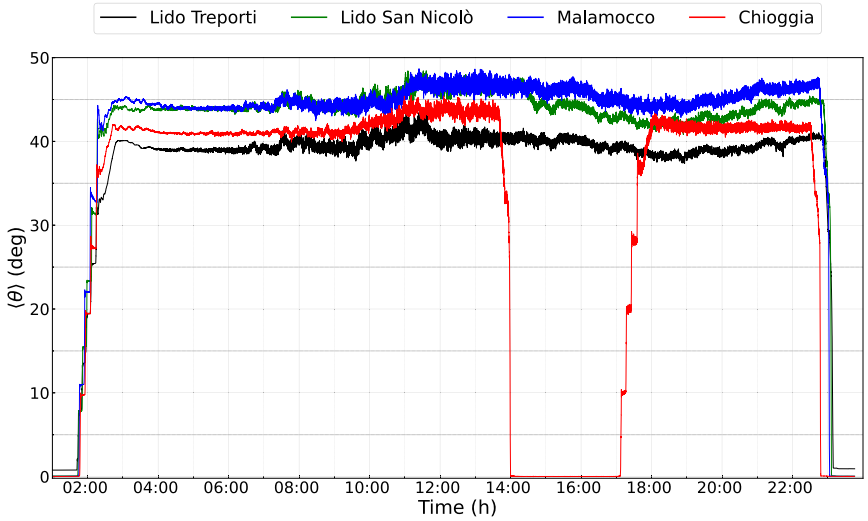

Fig. 7. Time series $\langle\theta\rangle$ of the four barriers.

some oscillations around the average working angle. Fig. 7 shows that in the time interval ranging from the raising of the barriers and the maximum seaside level peak (i.e. 9:40 h-10:30 h), the average working angle of the gates remained mostly constant. After 10:30 h and until about 11:30 h, a modest increase in the gates angles is visible. From 14:00 h to 19:00 h, the mean angle decreased. In this time interval, the levels increased, reaching the second peak around 19:00 h (Fig. 3 and Table 2). Towards the end of the day, the levels dropped again, causing a slight increase in the mean angle.

To quantify the movements of each gate, the time series of the oscillations have been analyzed in the time window 11:00 h–13:30 h. In order to focus only on the short period oscillations and to remove the low-frequency motions, mainly related to the gates raising and to the changing water levels, a high-pass filter with a cutoff frequency of 0.01 Hz has been applied. The filtered time series are shown in Fig. 8 panels *a, b* and *c* for gates 9, 10 and 11 respectively. Panel *d* of Fig. 8 shows for each gate the values of mean angle $\overline{\theta}_j^{150}$ and the standard deviation σ_j^{150} of each gate. The filtered time series have been processed using a method similar to the zero-crossing technique used for the surface waves, with the aim of identifying the amplitudes (a) of the oscillations of the gates. Statistical parameters such as the average ($\overline{a_\theta}$) and the average of the largest 33% ($\overline{a_{\theta 1/3}}$) amplitudes, are also calculated. The oscillations resulted to be quite uniform along the barrier, with a maximum value of $\overline{a_{\theta 1/3}}$ of the order of 1.5° and a mean $\langle\overline{a_{\theta 1/3}}\rangle$ of 1°, against a mean $\langle\overline{a_\theta}\rangle$ of 0.65°. To further quantify the magnitude of the gates oscillations, the vertical displacement (ζ) of the intersection of the still water level and the axis of the gate is calculated for each gate, using basic trigonometry. The same statistical parameters used for the angular oscillations are calculated for the displacements ($\overline{a_\zeta}$, $\overline{a_{\zeta 1/3}}$). The mean displacement $\langle\overline{a_{\zeta 1/3}}\rangle$ is 0.16 m and the maximum displacement $\langle\overline{a_\zeta}\rangle$ is of the order of 0.3 m and the minimum of 0.20 m.

One further point to be investigated is the differential oscillation between neighboring gates. Indeed, the ability of the barrier to efficiently disconnect the sea from the lagoon is enhanced if each gate, while oscillating, has an angular position not too different from the neighboring ones. Hydraulic performances are satisfactory when difference angles between neighboring gates are below approximately 15°, i.e. the maximum differential angle that ensures the differential rotation of neighboring gates is less than their width. To this end, Fig. 9 is introduced. It reports, the time series of the angles difference between a gate and the neighboring one: $\theta_j - \theta_{j-1}$ ($\theta_{10} - \theta_9$, panel *a*; $\theta_{11} - \theta_{10}$, panel *b*; $\theta_{12} - \theta_{11}$, panel *c*). Note that also here the calculation is performed using the high-pass filtered data of Fig. 8. Statistical parameters are calculated and reported in the bottom right panel, where the average and the standard deviation of the absolute value of the difference are plotted for each couple of neighboring gates. It shows also the maximum and minimum values of the $\theta_j - \theta_{j-1}$ time series for each gate, indicated at side of each bar. The pair of gates 13–12 shows the highest mean values, with a differential oscillation below 0.5° and standard deviation smaller than 1°. The recorded values are well below the threshold of 15° mentioned before: we therefore conclude that during this event the hydraulic barrier performance was satisfactory.

4. Analysis of dynamical response of the Chioggia inlet and barrier

The natural modes of the barrier are presented in Section 4.1. The modal analysis of the Chioggia inlet in Section 4.2, while the EOF analysis is highlighted in Section 4.3.

4.1. Natural modes of Chioggia barrier

The $N-1$ periods of the natural modes $G_j (j = 1, \ldots, N-1)$, with $N = 18$ the number of gates of the barrier have been estimated by applying the model of Li and Mei (2003b). The model allows the reproduction of a finite length barrier of inclined gates, with different water levels on both sides of the barrier. This results from combining the approaches of Li and Mei (2003a) for a barrier of finite length vertical gates and the hybrid element method for an infinitely long barrier of inclined gates of Liao and Mei (2000).

The modal shape $\beta(x)$ of each mode along the x-axis spanning the barrier width, is a piecewise replica of a cosine curve:

$$\beta_j = \int_{X_j} \cos\left(\frac{2K\pi x}{L}\right) \mathrm{d}x = \frac{L}{2K\pi}\left(\sin\frac{2Kj\pi}{N} - \sin\frac{2K(j-1)\pi}{N}\right), \qquad (1)$$

where β_j is the normalized rotation of gate j of width $X_j = L/N$, with N number of gates and L the barrier width and $2K$ is an integer so that there are K half modal wavelengths along the barrier. A detailed description of the characteristics of the modes is given in Li and Mei (2003a).

Once the geometrical and inertial characteristics of the gates and the water levels at the inlet are known, the eigenfrequencies can be evaluated by solving the eigenvalue problem for the discrete dynamical system made of all the gates of the barrier. Changes in head difference Δh, as well as changes in equilibrium angles, can lead to variations in the periods of the jth modes G_j. The influence of such variations has been investigated. It has been found that with no sea-lagoon level

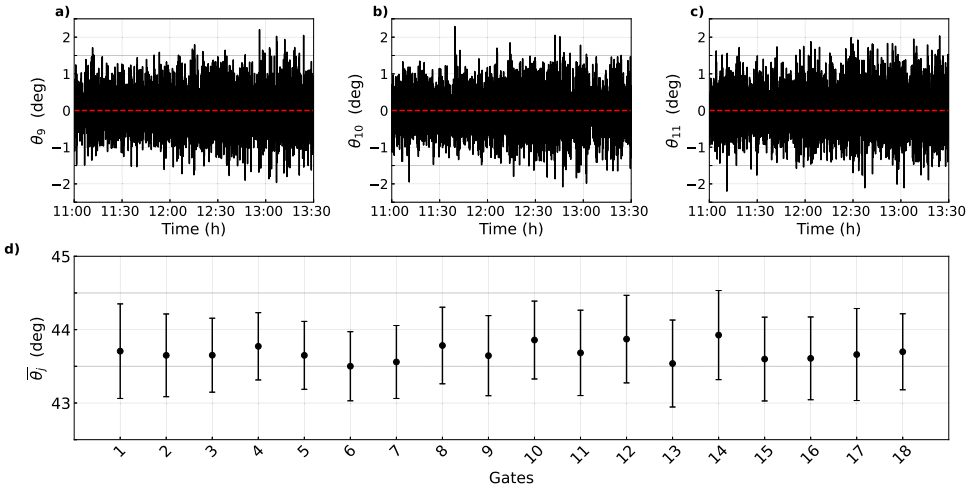

Fig. 8. Time series of the high-pass filtered oscillations of gates 9 (panel a), 10 (panel b), and 11 (panel c), for the Chioggia barrier in the time interval 11:00 h-13:30 h. Panel (d) reports the statistical parameters, where the mean and the standard deviation of the inclination angles are plotted for each gate.

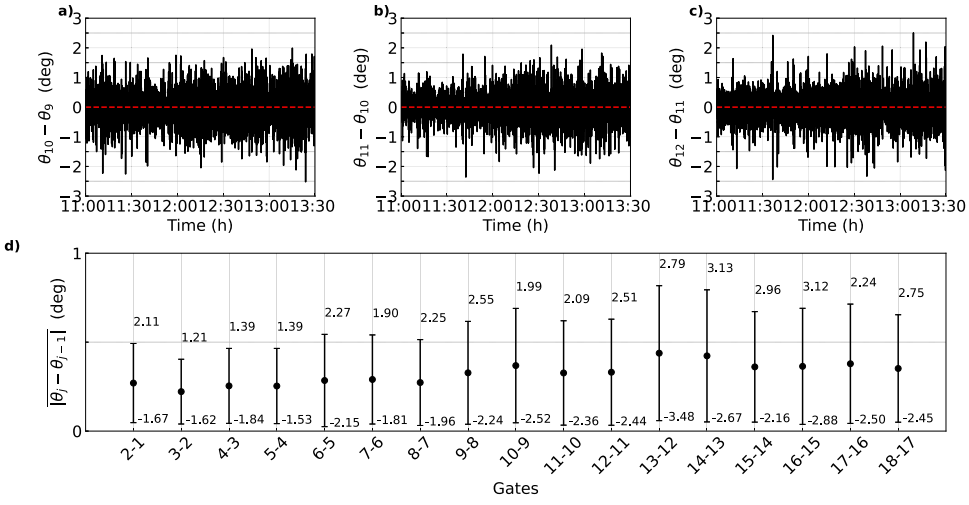

Fig. 9. Time series of angle differences between neighboring gates (panel a: gates 10-9; panel b: gates 11-10; panel c: gates 12-11) of the Chioggia barrier in the time window 11:00 h–13:30 h. Panel (d) reports the statistical parameters, where the average and the standard deviation of the absolute value of the difference are plotted for each couple of neighboring gates.

difference ($\Delta h = 0$) the natural periods are only slightly influenced by variation in water levels, with a 5% average rate of change $T_{h=13}/T_{h=11}$. Moreover, it was found that a variation in the equilibrium angle within a range of 2° (the range of recorded variability of the mean angle) has no effects on the periods calculated.

Assuming a constant h_L = 11.6 m, Fig. 10 shows the dependence of the natural periods T of the G_j modes on Δh. An increase in Δh corresponds to an increase of the natural periods (increase in added mass). The trends of the natural periods of all the modes are plotted in Fig. 10*a*, while modes ranging from G_1 to G_{12} are enlarged in Fig. 10*b*. For the first three modes, when Δh = 2.5 m, the periods significantly increase by about 25% compared to the case of $\Delta h = 0$ ($T_{\Delta h=2.5}/T_{\Delta h=0}$ = 1.25). The percentage increase is lower for higher modes, e.g. for the G_{10} mode $T_{\Delta h=2.5}/T_{\Delta h=0}$ = 1.20. Even lower increase rates are found for modes G_{16} and G_{17} (see Fig. 10*a*), e.g. $T_{\Delta h=2.5}/T_{\Delta h=0}$ = 1.08 for G_{17}.

During the event of November 22nd both the levels and the gates inclination fluctuated (Figs. 3 and 7). Accordingly, also the natural mode periods changed with Δh. To properly evaluate the dynamical response of the barrier, an appropriate time interval has been chosen: sufficiently short to minimize variations in Δh, yet long enough to enable feasible spectral analysis, as will be discussed in subsequent sections. In particular, the natural periods of the Chioggia barrier have been estimated referring to the mean levels recorded between 12:00 h and 12:30 h, considering h_S = 12.12 m, h_L = 11.81 m (Δh = 0.31 m) and a mean angle $\langle \bar{\theta}^{30} \rangle$ of 43.8°. The modal shapes and the calculated modal periods of the G_j modes of the Chioggia inlet are plotted in Fig. 11. The natural periods (white squares) and the eigenfrequencies (black dots) are plotted in the bottom right panel of Fig. 11. The estimated period of the first mode G_1 = 10.75 s is consistent with the previous experimental findings of the model tests (1:60, 1:30 and 1:10 scale model tests). The tested conditions do not exactly coincide with those that occurred during the event; however, at h_S = 11.6 m and Δh = 0 m the mean period of the first mode was measured as 10.7 s (Consorzio-Venezia-Nuova, 2002c).

4.2. Modal analysis of the Chioggia inlet

It is expected that the waves and barrier dynamics can be influenced by the excitation of some of the natural modes of the elevation of the free surface in the inlet. In order to help the interpretation of the barrier dynamics an a priori analysis of the resonant modes has been carried out and presented in this section.

The analysis has been based on the technique introduced by Bellotti (2020), Bellotti et al. (2012a,b) and Bellotti and Romano (2017). It

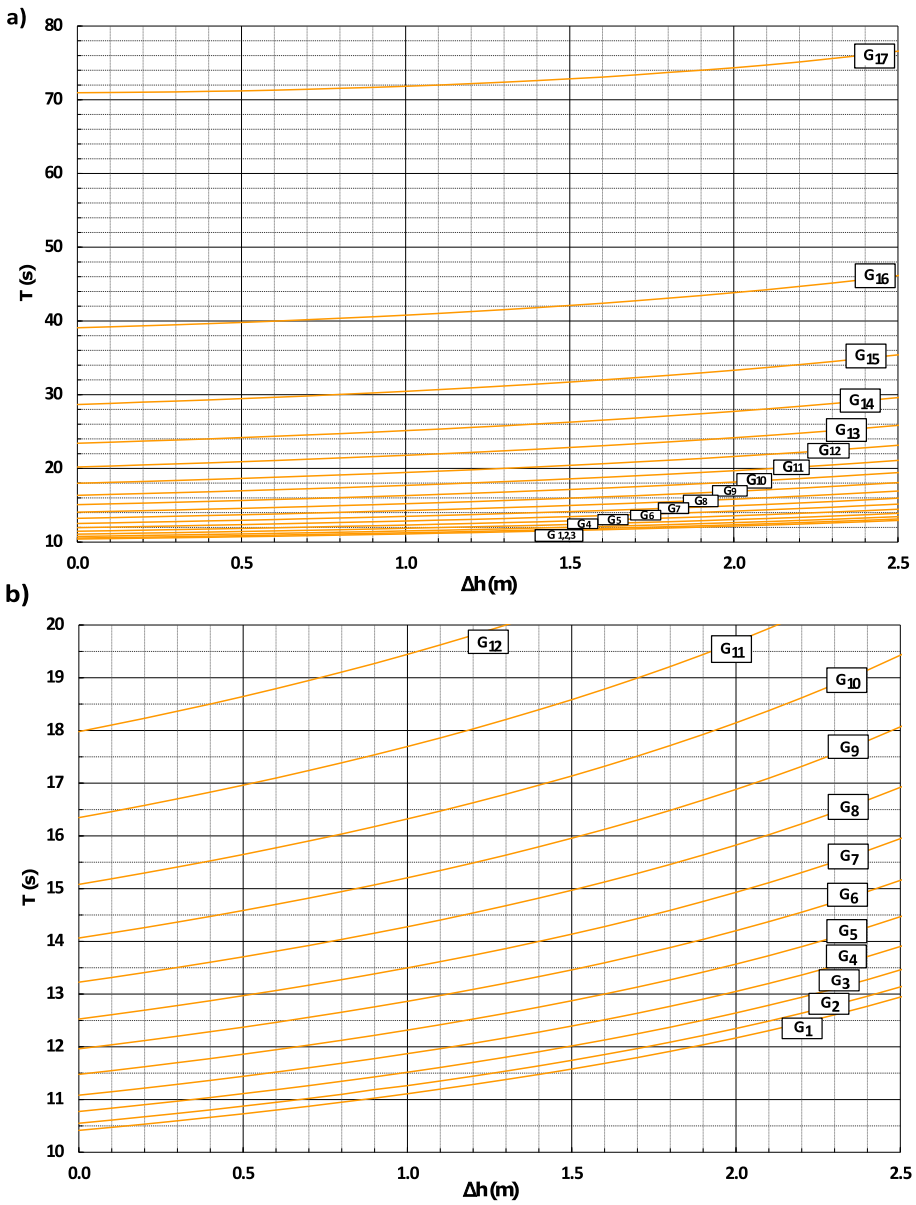

Fig. 10. Relationship between the natural periods and the head difference Δh for all the modes (panel a) and for modes from G_1-G_{12} (enlarged panel b).

relies on the solution of an eigenvalue problem that stems from the homogeneous linearized long waves equation, converted by means of the finite element technique into a system of ordinary differential equations in time. The computational domain and the bathymetry used for the analysis are represented in Fig. 12. The average size of the FEM elements is 200 m and the number of degrees of freedom is 5866. At the boundaries that represent the coastline, maritime structures and the MoSE barrier, mathematical conditions that reproduce full reflection of the waves are applied. It should be noted that the barrier gates are considered fixed and their actual oscillations do not generate feedback into the system. At the semicircular boundary that separates the computational domain from the semi-infinite open sea, an approximate radiation condition is used. This introduces a source of damping into the mathematical problem; therefore, the resulting eigenvalues are complex. Note that the model equations are frictionless, thus implying a slight overestimation of the modal frequencies. The simulation was carried out for a water depth of 12.5 m, i.e. 1.5 m above the mean sea level.

The result of the analysis is a set of eigenvalues and eigenvectors. The former represents the frequency of the free oscillations of each mode. Since these are complex, the real part describes the damping associated to each mode. The latter represents the spatial normalized shape of the inlet channel modes C_i, $i = 1, 2, \ldots$. Figs. 13, 14 report the first 16 most relevant modes, ordered in terms of their decreasing periods (increasing natural frequencies). Figs. 13 and 14 are shown for the phase at which the maximum difference between positive and negative values of the eigenvector is attained.

The modes C_1, C_3, C_5, C_6 are the 0th, 1st, 2nd and 3rd order longitudinal modes, respectively. They are of special interest for the following analysis, since, due to their spatial shape, they can force an in-phase response of the barrier. Mode C_1 is the 0th order longitudinal mode of the inlet, as one nodal line appears at the entrance and the anti-node is located along the barrier. Mode C_3 is the 1st order longitudinal mode, with one nodal line at one quarter of the inlet length from the barrier and one nodal line at the entrance. The mode C_5 is the 2nd order longitudinal mode, the mode C_6 is 3rd. It is worth noticing that some modes (e.g. C_2, C_5, C_{10}, C_{14}) do exhibit a relevant interaction with the offshore breakwater placed to shelter the inlet from south-east. Finally, C_4 is the Helmholtz mode of the navigational bay.

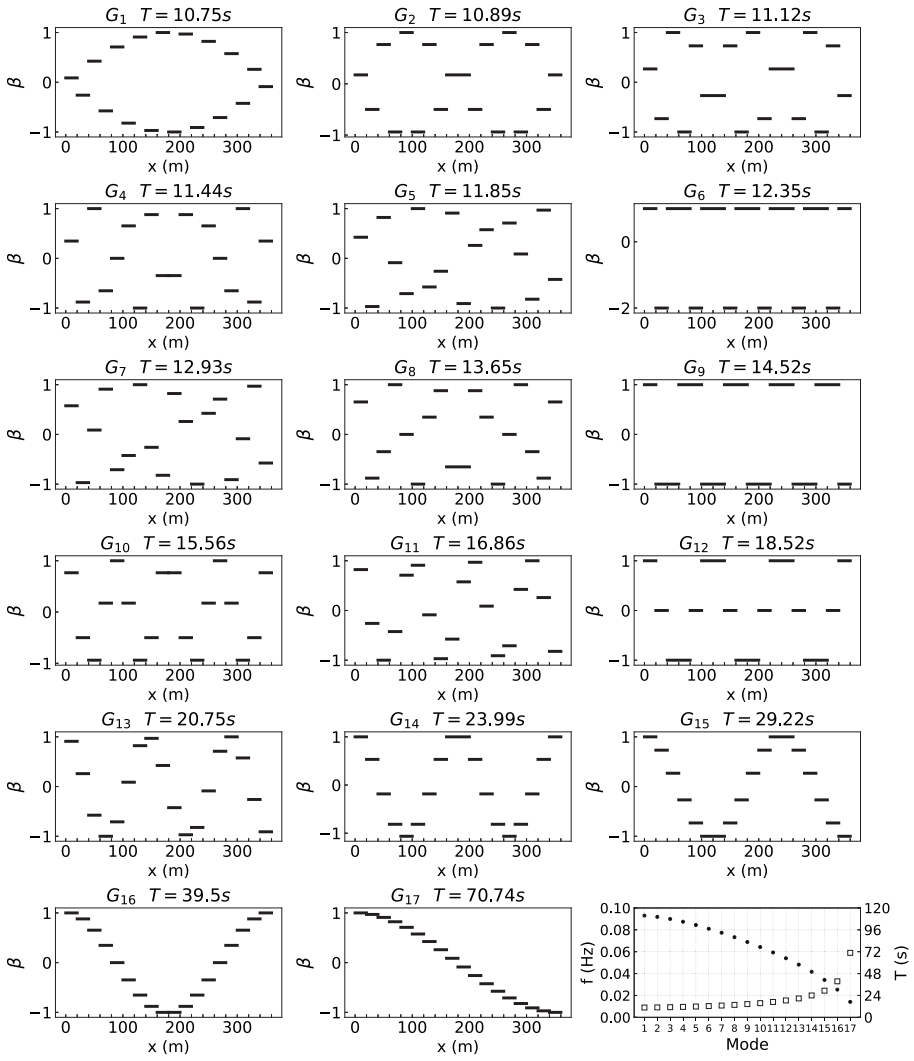

Fig. 11. Modal shapes and periods of the Chioggia barrier. In the bottom right panel the eigenperiods and eigenfrequencies of the barrier.

4.3. Empirical Orthogonal Functions (EOF) analysis

EOF analysis is a mathematical method used to investigate the spatial variability of a dynamical system. Spatially varying measured time series are projected on an orthogonal basis consisting of a number of eigenfunctions equal to the number of spatial variables in the system (in this case $N = 18$ gates). Each of these spatial orthogonal functions represents a contribution to the total variability of the system. Through EOF analysis, it is possible to empirically identify the basis of orthogonal eigenfunctions (EOFs) and their associated time-varying components.

In the case of the gates barrier, the data set $\boldsymbol{\Theta}(x,t)$ of the recorded angles of the N gates vary in space (x) and in time (t); the space coordinate x is indeed represented by the integers from 1 to N, which individuate the ordered position (left to right) of each gate along the barrier axis of Fig. 11. For simplicity, in the following, we keep the generic notation x. EOF analysis requires solving the eigenvalue problem for the covariance matrix of the system $C = \widetilde{\boldsymbol{\Theta}}^T\widetilde{\boldsymbol{\Theta}}$, where $\widetilde{\boldsymbol{\Theta}}$ is the data set $\boldsymbol{\Theta}(x,t)$ adjusted around the mean angle of each jth gate $\bar{\theta}_j^{\tau}$, in index notation each one of the $j = 1,\dots,N$ vectors that form the matrix $\widetilde{\boldsymbol{\Theta}}$ is :

$$\tilde{\boldsymbol{\theta}}_j\left(t_m\right) = \boldsymbol{\theta}_j\left(t_m\right) - \bar{\theta}_j^{\tau} \tag{2}$$

The eigenvalue problem is formulated as follows:

$$\mathbf{C\Gamma} = \lambda\mathbf{\Gamma}, \tag{3}$$

where λ is the generic eigenvalue and $\mathbf{\Gamma}$ is the corresponding eigenvector. The relative variance of the gates array system associated with the nth eigenvalue λ_n of the problem is defined as:

$$\sigma_n^2 = \frac{\lambda_n}{\sum_{j=1}^{N}\lambda_j}, \quad n = 1,\dots.N, \tag{4}$$

and represents the percentage of the total energy of the gates array associated with the nth spatial pattern, i.e. with the eigenvector $\mathbf{\Gamma}_n$ (Panizzo et al., 2006).

Due to the orthogonality of the eigenvectors $\mathbf{\Gamma}_n$, the original dataset of measurements can be expressed through a finite series expansion in terms of the eigenvectors $\mathbf{\Gamma}_n$ with their respective time-dependent components $\alpha_n(t)$, so that at each generic time t_m it results:

$$\widetilde{\boldsymbol{\Theta}}(x,t_m) = \sum_{n=1}^{N}\alpha_n(t_m)\mathbf{\Gamma}_n(x), \quad m = 1,\dots,M. \tag{5}$$

The time evolution $\alpha_n(t)$ of each EOF can be obtained by projecting the original dataset $\widetilde{\boldsymbol{\Theta}}(x,t_m)$ on each eigenvector:

$$\alpha_n(t) = \widetilde{\boldsymbol{\Theta}}(x,t_m)\mathbf{\Gamma}_n(x). \tag{6}$$

Among the N EOFs, those with higher relative variance are associated with higher energy content and, consequently, they are the most significant in describing the spatial variability of the system.

Fig. 15 shows the first three EOFs ($n = 1,2,3$) extracted from the time series of the $N = 18$ Chioggia gates, measured from $t = 11{:}00$ h

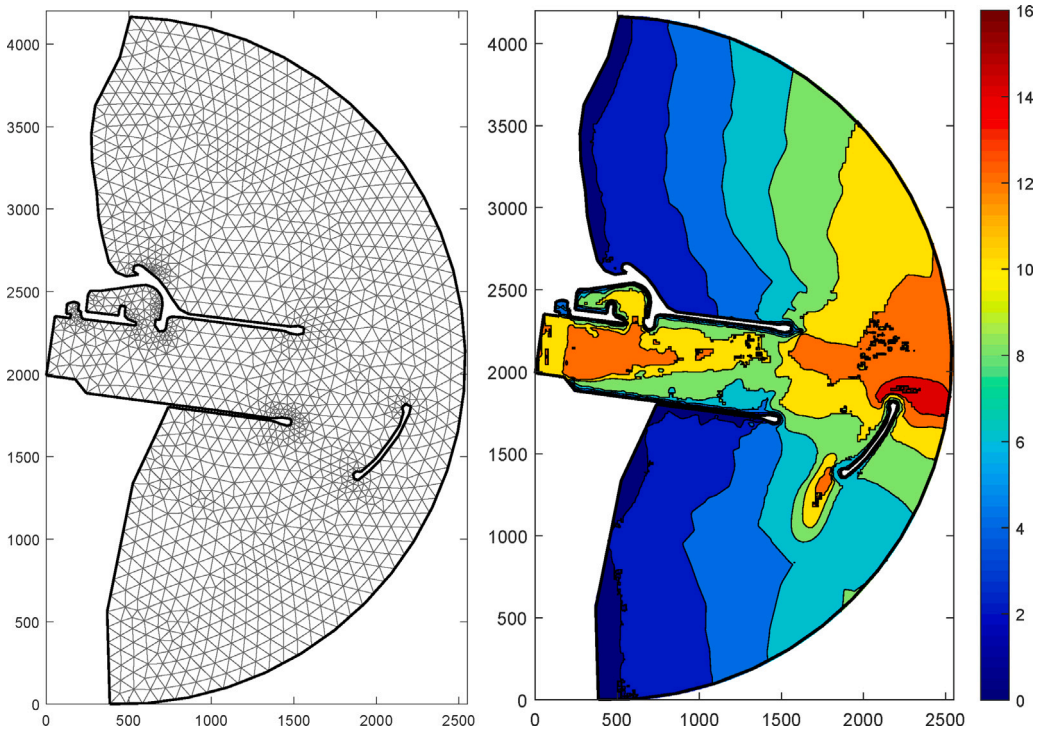

Fig. 12. Finite element mesh (left) and bathymetry (right) used for the modal analysis. The colorbar indicates the water depth in meters.

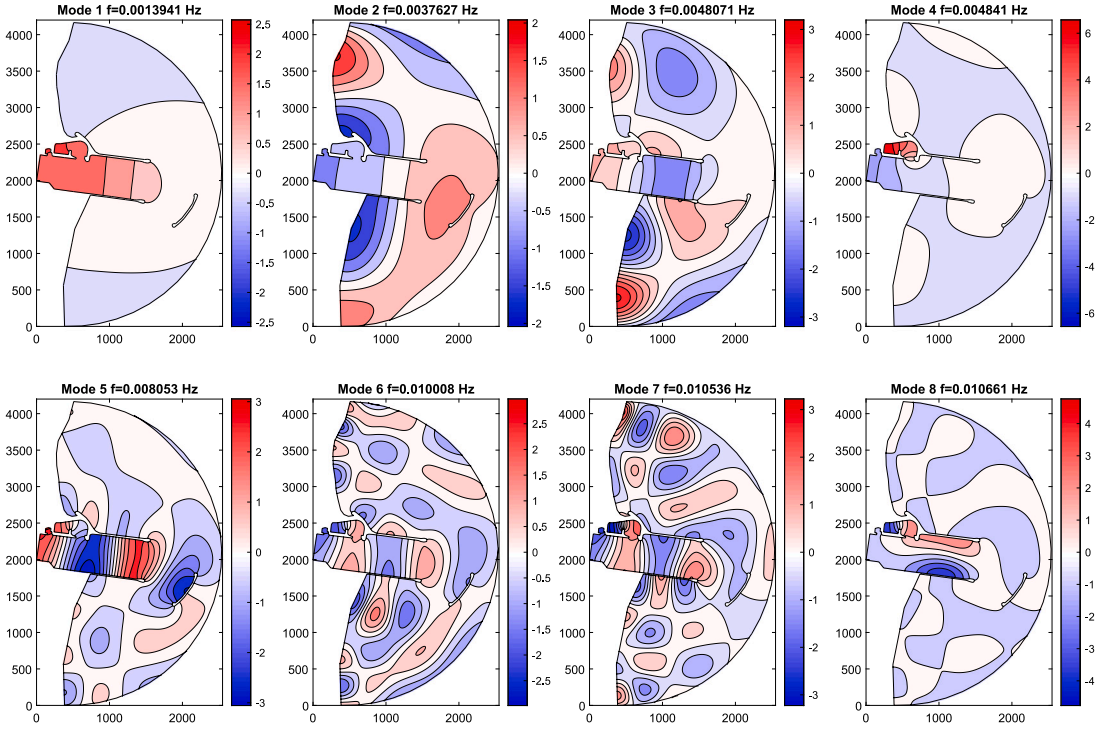

Fig. 13. Surface elevation of the first set of eight normal modes of the Chioggia inlet. x and y coordinates are in meters and refer to a local model reference system. The colorbars indicate the dimensionless surface elevation.

to t = 13:30 h on November 22nd ($M = 9000$). Each row of the plot of Fig. 15 represents a different EOF as follows: the first panel on the left depicts the EOF spatial pattern; the middle panel illustrates the specific value of λ_n (red dot) and the associated value of σ_n^2. The right panel displays the power spectral density (PSD) of the specific component $\alpha_n(t)$.

The cumulated relative variance of the first three ($n = 1, 2, 3$) EOFs is $\sigma_n^2 = 0.68$, i.e. 68% of the total energy; the first $n = 1$ EOF contributes

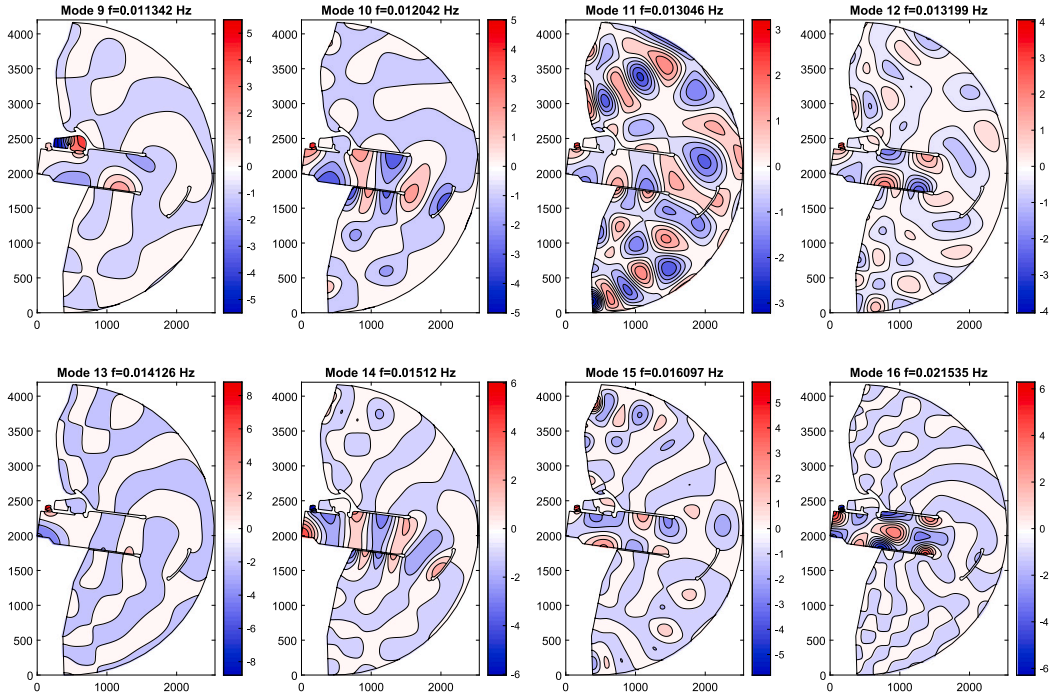

Fig. 14. Surface elevation of the second set of eight normal modes of the Chioggia inlet. The colorbars indicate the dimensionless surface elevation.

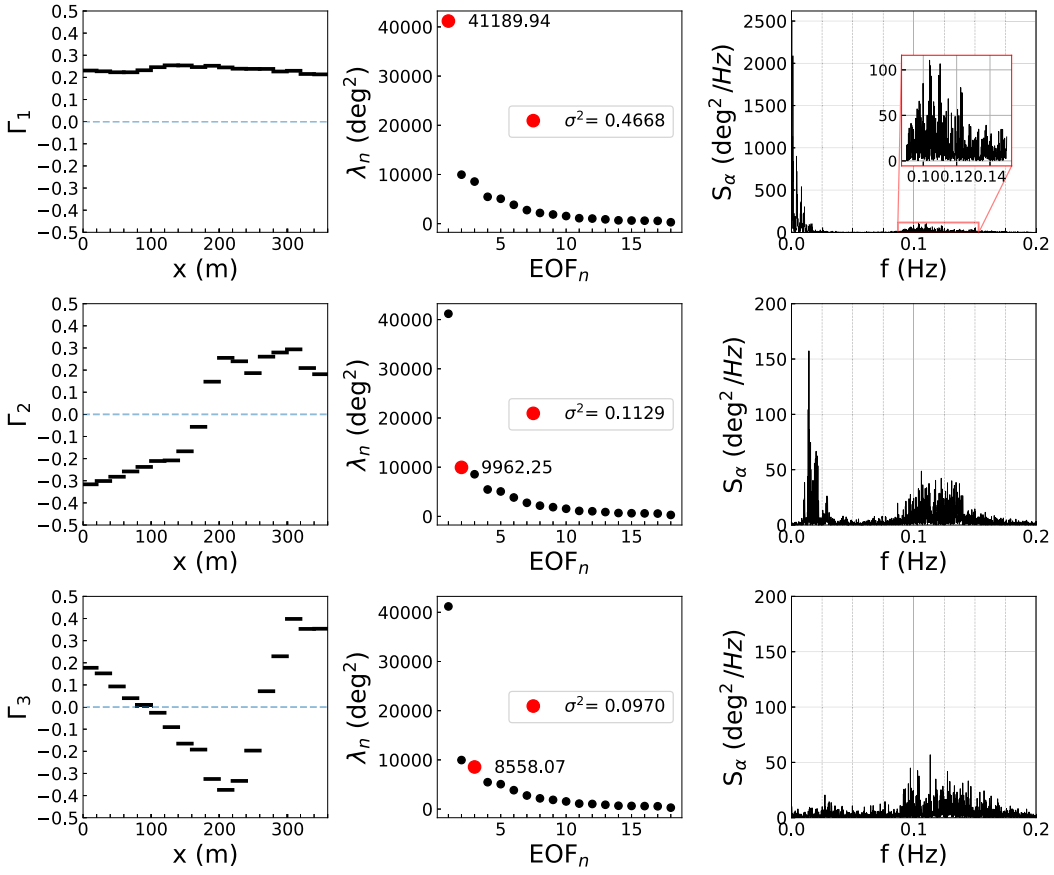

Fig. 15. EOFs of the gates oscillations at Chioggia.

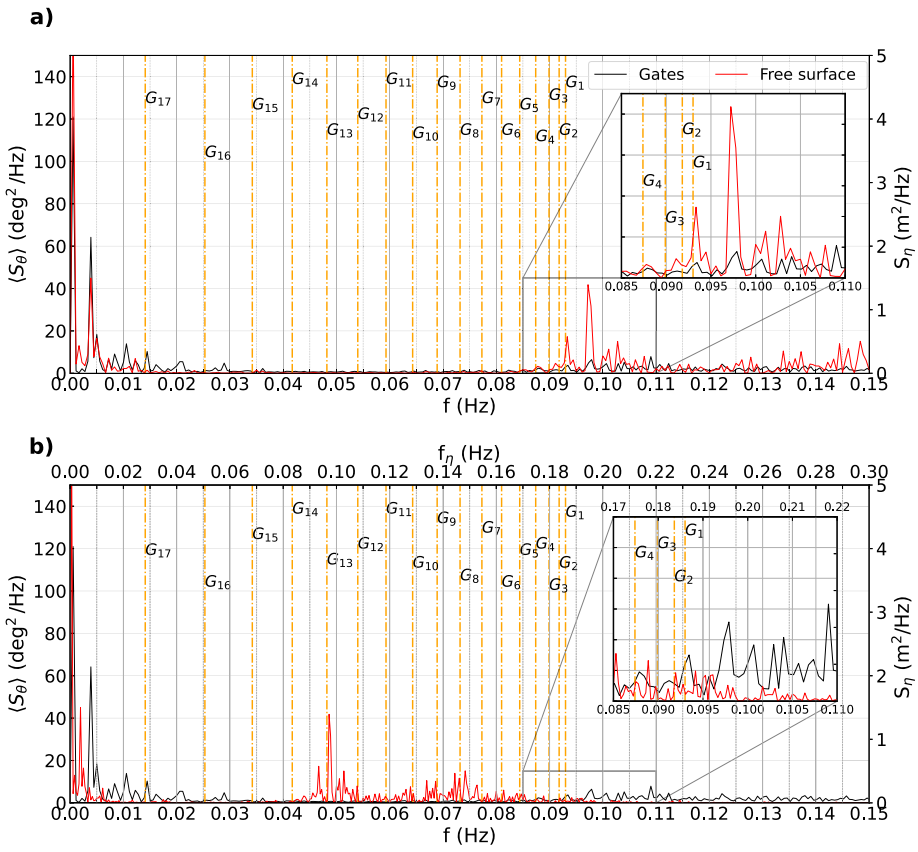

Fig. 16. Panel (a). The average energy spectrum of the gates and of the free surface. The orange dashed lines represent the frequencies of the natural modes of the barrier. Panel (b). As above, but wave spectrum is plotted using a distorted x-axis ($f/2$).

to the total energy of the system by 47%. EOF1 represents a spatially in-phase mode, the empirical modal shape never crosses zero: the gates oscillate in phase. The temporal behavior of all three empirical modal shapes exhibits two distinct spectral peaks (third column in Fig. 15): a long period oscillation (around 100 s) and a shorter period oscillation (around 10 s).

5. Analysis and discussion

In this section the magnitude and the nature of the barrier and gates oscillations are investigated. Firstly, the potential excitation, both synchronous and subharmonic, of the barrier natural modes by short waves is analyzed. Then, the low-frequency barrier oscillations driven by the resonant modes of the inlet are discussed. Finally, the EOF analysis is applied to investigate the relationship between the forcings and the spatial shape of the barrier natural modes.

The analysis of the excitation mechanisms of the barrier is carried out on the basis of the spectral analysis of waves and gates' oscillations. Reference is made to Fig. 16, obtained using the data in the time window from 12:00 h to 12:30 h of November 22nd. The considered time window has been selected as it exhibits a relatively small variation of the water level, specifically $\Delta h = 0.31$ m and $h_S = 12.12$ m, and at the same time the wave height is $H_{m0} = 0.9$ m. In the considered time interval, the averaged inclination angle of the barrier $\overline{\langle\theta\rangle}^{30}$ is 43.8°, with an average standard deviation $\left\langle\sigma^{30}\right\rangle$ of 0.7°. In Fig. 16 the red line shows the spectrum of the free surface elevation measured by the ADCP, while the black line refers to the spectrum of the gates oscillations. Specifically, the latter is obtained as the average of the spectra of each gate and can be regarded as the spectrum of the overall energy pertaining to the barrier.

While in the upper panel *(a)* for each frequency the corresponding wave and gates energy content is shown, in the lower panel *(b)* frequencies of the wave spectrum are divided by a factor of 2 and are marked on the secondary axis above, indicated by f_η. This allows a simple and direct evaluation of the existence of synchronous (panel *a*) and subharmonic (panel *b*) excitation mechanisms. Moreover, the frequencies of the natural modes of the barrier (see Fig. 11), are reported in both panels as orange dashed lines.

The spectra reported in Fig. 16 show that the wave energy is concentrated in two distinct frequency bands. The first is in the range 0.00–0.02 Hz; it is associated with resonant long waves of the inlet and it is discussed later in this section. The second band is in the range 0.08–0.15 Hz and represents the short waves. By comparing the wave and barrier spectra in panel *a*, it appears that in the range 0.09–0.105 Hz, there exists some synchronous correspondence between the energy peaks of the waves and of the barrier. The highest energy peaks of waves and gates occur at about 0.0975 Hz. This indicates that a synchronous response of the barrier is forced by the short waves. As far as the natural modes of the barrier are concerned, no energy is found at their frequencies, apart from the small peak that occurs at G_1. Inspection of panel *b* of Fig. 16 reveals that no barrier energy is found at the frequencies of the potential subharmonic components of the short waves. This is an indication of the fact that, for this event, no subharmonic resonance has been excited. This might be consistent with the theoretical findings of Sammarco et al. (1997a): they pointed out that nonlinear subharmonic resonance can only be triggered if the wave energy is larger than some critical threshold values. Possibly, during the event the wave energy was not enough to activate the response. One further important point to be kept in mind is that the gates' motion is likely to be further damped by the feedback control system, which regulates the influx of air in order to maintain the design inclination angle of the gates.

After the analysis of the high frequency oscillations, we turn to the low frequencies. To this end the spectral analysis is carried out on a time window of longer duration (11:00 h-13:30 h). This allows to

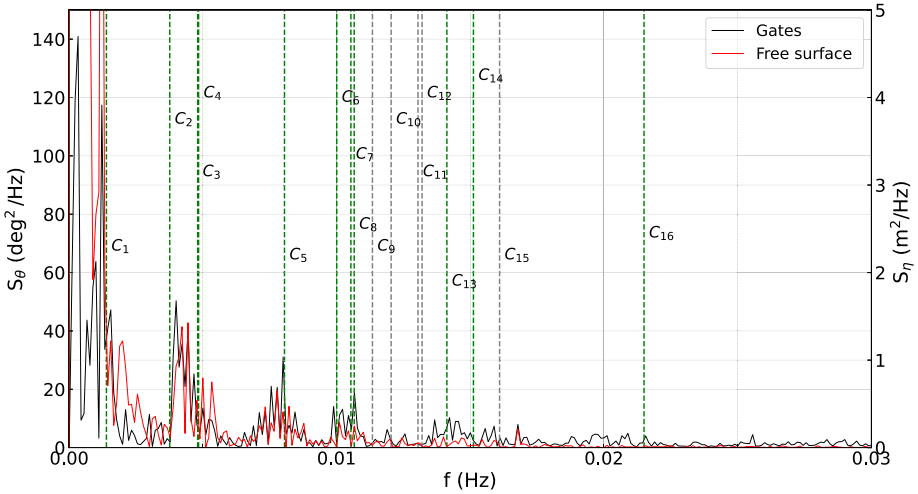

Fig. 17. Spectral analysis of the barrier and the free surface PSD. The green dashed lines represent the frequencies of the inlet modes that are likely responsible for the excitation of the gates barrier.

increase the frequency resolution, which is important to explore the low frequencies range. In the selected time window the level h_S changed from 12.5 m to 11.76 m, and Δh varied from 0.86 m to −0.11 m, while H_{m0} is of 0.9 m. The average inclination angle of the gates remains almost constant (Fig. 7) at about 43.9°, with an average standard deviation $\langle \sigma^{150} \rangle$ of 0.7°.

The analysis of the low-frequency barrier motions is carried out on the basis of the spectral analysis reported in Fig. 17, which is similar to the panel *a* of Fig. 16 apart from the used time window which is now larger. The frequencies of the modes of the lagoon inlet (see Figs. 13 and 14) are reported as vertical dashed lines. The modes with large amplitudes at the barrier are represented by green lines, while for the others gray is used. Inspection of Fig. 17 reveals a correspondence between some of the inlet modes natural frequencies and some of the spectral peaks of the barrier motion. This suggests, again, that a synchronous forcing mechanism is active. These peaks are located at frequencies quite close to those of some of the natural modes evaluated through the modal analysis technique. Specifically, some longitudinal modes (C_1, C_2, C_3, C_5, C_6, C_7, C_{14}), the Helmholtz mode of the navigational bay (C_4) and some cross-modes (C_8, C_{16}) of the inlet appear to be amplified due to inlet resonance and therefore appear to force barrier motions. Since the forcing mechanism is likely to be synchronous and driven by long-waves resonance, it is interesting to explore the relationship between the spatial shape of the inlet modes and the corresponding shape of the barrier motions. This is investigated through the EOF analysis technique. Specifically, the spectra of the three first EOFs (Fig. 15) are here analyzed in more detail and magnified in Fig. 18. On each of the three subplots of Fig. 18 the frequencies of the relevant natural modes of the inlet are also reported, using vertical dashed green lines. These have been selected among those that have a spatial variation at the barrier that resembles the shape of the considered EOF. Similarly, the frequencies of the relevant natural modes of the barrier are plotted using vertical orange bands, enveloping the variability of the frequency in view of the variation of water level in the considered time window (see Fig. 10). It is interesting to note that the comparison of the EOFs, inlet and barrier responses, although derived via different methods and forcings, exhibit some similarities. In fact, the comparison of the modal shapes of the EOFs in Fig. 18 and the theoretical natural modes in Figs. 11 (barrier) and 13 (inlet) reveals a similarity between the EOF1 and the in-phase inlet mode C_1, the EOF2 and G_{17}, just as the EOF3 resembles a mix between G_{16} and G_{15}.

The EOF1, reported in the panel *a* of Fig. 18, represents gates oscillations that are mostly uniform along the barrier. According to the spectra, these oscillations appear to be forced predominantly by the resonant long waves of the inlet, although it is not possible to prove that a causal link exists. Given the spatial distribution of the oscillations, it is likely that the longitudinal inlet modes are those responsible for these oscillations. In fact, all the spectral peaks correspond to frequencies of inlet longitudinal modes. Also the Helmholtz mode C_4 of the navigational bay induces almost constant free surface elevation at the barrier and forces this specific EOF.

The EOF2 is analyzed in the panel *b* of Fig. 18. It should be noted that its energy content is about 25% than that pertaining to EOF1. According to EOF2, the gates are not uniformly oscillating across the inlet, rather the shape resembles, although not perfectly, that of half of a cosine wave. The energy peaks in the spectrum are associated with the crossed natural modes of the inlet; at the barrier they exhibit a free surface elevation variation which appears similar to the shape of the EOF. The largest peak has a frequency that is very close to those of the inlet mode C_{13} and of the barrier mode G_{17}. However, it should be noted that the two modes share the same frequency: 0.0141 Hz (see Figs. 11, 13 and 14). Furthermore, a small energy peak is found at the frequency of the barrier mode G_{16}. It seems therefore that, for this EOF, the barrier oscillations are dominated by the resonant modes of the inlet, and by the longest Chioggia barrier mode.

As one proceeds with the analysis of the following EOFs (see example of EOF3 in panel *c* of Fig. 18) no significant energy peaks appear in the spectrum. A small energy peak appears located in between the frequencies of the barrier modes G_{16} and G_{15} in agreement to the observation about EOF3 modal shape and to its lower energy content (σ_n = 9.7%, third row in Fig. 15).

6. Concluding remarks

The analyses presented in this paper focus on the dynamical response of the MoSE barriers to the storm event of November 22nd, 2022, the most important storm surge event since the beginning of operations in 2020. Persistent *Scirocco* winds, combined with low pressure and astronomical tide, significantly increased the surge levels. As the sea state average direction shifted towards *Bora*, waves significantly penetrated into the inlet, reaching the barriers. This resulted in combined surge and waves acting on the barrier at the same time, leading to a potential critical condition for the system. In this study, the following time series have been analyzed: sea level measured inside the lagoon and in front of the barriers, ADCP measurements in front of the barriers, gates angular position measured by electronic inclinometers.

First of all, for the specific storm event considered, the MoSE system has proven to be able of limiting the rising of the waters inside the

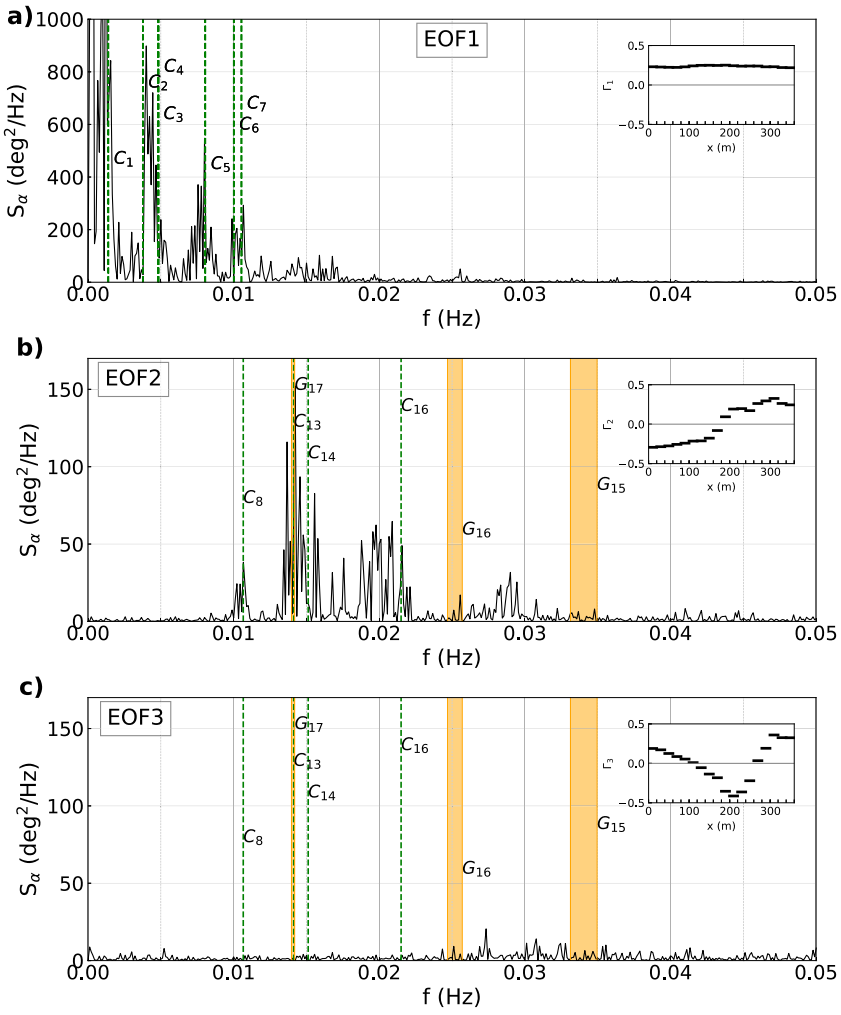

Fig. 18. Panel (a) represents the EOF1 PSD, panel (b) the EOF2 PSD and panel (c) the EOF3 PSD. The green dashed lines represent the frequency of the inlet modes. The orange bands represent the calculated eigenfrequencies relative to the excursion of Δh between 11:00 h and 13:30 h.

lagoon and to efficiently protect the city of Venice from flooding. According to the analyses carried out, during the considered storm event, the gates have been affected by moderate oscillations around their design working position (on average smaller than 1.0° during the operation interval considered) and the angle difference between neighboring gates is overall such that the barrier of Chioggia guarantees satisfactory hydraulic disconnection between the sea and the lagoon.

In order to investigate in detail the nature of these small amplitude oscillations, the Chioggia inlet has been selected for an in-depth analysis. To support the interpretation of the data, two models have been applied to calculate the frequencies and the shapes of the natural modes of the system. The first looks at the resonant modes of the barrier (Li and Mei, 2003b). The application of the model has confirmed that the frequencies of the barrier resonant modes depend also on the difference in water level between the sea and lagoon. The second considers the resonant long waves of the inlet through a modal analysis of the long waves equation (Bellotti, 2020).

By analyzing the spectrum of the barrier oscillations, it has been found that, for the considered event, two distinct energy bands exist: one forced by short waves and the other by low-frequency waves. The latter appears more relevant than the former. Comparison of waves and barrier spectra in the high-frequency band, reveals that the excitation mechanism is synchronous, while subharmonic resonance appears not to be activated during the event studied. As far as the low-frequency band is concerned, it is found that several longitudinal and crossed modes of the inlet may be the most probable cause of the barrier movements during the event studied. These conclusions have been driven by the EOF analysis, that has helped interpretation of the spatial shape of the barrier modes. It results that the major contribution to the gates response is likely due to the longitudinal modes, which are detected in the most energetic EOF1. It is important to highlight that, although only one single event is analyzed, these findings have a general meaning for two reasons: (I) the cyclogenesis and evolution of the storm event of November 22nd, 2022, i.e., the most important storm surge event since the beginning of operations in 2020, are archetypal conditions to which the MOSE system will be prone in the future; (II) the study provides the interpretation of complex phenomena by studying a representative event applying a combination of state-of-the-art techniques (i.e., EOF, inlet and gates modal, and spectral analyses).

To summarize, the oscillations of the gates of the MoSE around their working position appear to be limited during the considered intense event. This observed response suggests that the MoSE system behaved as designed during the considered storm event which we recall has been the strongest since beginning of operations. Further verification of the mechanical response will be conducted if in the future more energetic events might occur. The stability of the system may have been further improved by the feedback system that, controlling in real-time the position of each gate, introduces an extra source of damping. However, since a single storm event is investigated it is not possible to provide general conclusions on the damping capabilities of the feedback system.

Future research will consider more detailed data that will become available to further evaluate the efficiency of the MoSE system and provide more insight into the physical mechanisms that drive the oscillations of the gates.

CRediT authorship contribution statement

Paolo Sammarco: Writing – review & editing, Writing – original draft, Supervision, Project administration, Methodology, Investigation, Funding acquisition, Formal analysis, Conceptualization. **Piera Fischione:** Writing – review & editing, Writing – original draft, Validation, Methodology, Investigation, Funding acquisition, Formal analysis, Data curation, Conceptualization. **Alessandro Romano:** Writing – review & editing, Writing – original draft, Validation, Supervision, Methodology, Investigation, Formal analysis, Conceptualization. **Giorgio Bellotti:** Writing – review & editing, Writing – original draft, Validation, Supervision, Methodology, Investigation, Formal analysis, Conceptualization. **Sergio Dalla Villa:** Validation, Supervision, Software, Resources, Data curation, Conceptualization.

Declaration of competing interest

The authors declare the following financial interests/personal relationships which may be considered as potential competing interests: Paolo Sammarco reports financial support was provided by Consorzio Venezia Nuova S.p.A. - Provveditorato interregionale per le OO.PP. Veneto-Trentino Alto Adige- Friuli Venezia Giulia. If there are other authors, they declare that they have no known competing financial interests or personal relationships that could have appeared to influence the work reported in this paper.

Data availability

The authors do not have permission to share data.

Acknowledgments

Research is conducted under the Grant to the University of Rome "Tor Vergata" *AVV.12 – Sistema MoSE - Avviamento - Misure in campo per la valutazione dell'interazione tra moto ondoso e paratoie* from Consorzio Venezia Nuova S.p.A. - Provveditorato interregionale per le OO.PP. Veneto-Trentino Alto Adige- Friuli Venezia Giulia. The data used in this study are provided by Consorzio Venezia Nuova (CVN).

References

Adami, A., De Girolamo, P., Noli, A., Venuti, A., 1995. Harbour resonance induced by incident irregular short waves: Influence of scale effects on the resonance of the chioggia inlet physical model. In: Excerpta of the Italian Contributions to the Field of Hydraulic Engineering. Vol. 9, pp. 7–40.

Adamo, A., Mei, C.C., 2005. Linear response of venice storm gates to incident waves. Proc. R. Soc. Lond. Ser. A Math. Phys. Eng. Sci. 461, 1711–1734.

Alberti, T., Anzidei, M., Faranda, D., Vecchio, A., Favaro, M., Papa, A., 2023. Dynamical diagnostic of extreme events in Venice lagoon and their mitigation with the MoSE. Sci. Rep. 13 (1), 10475, Nature Publishing Group UK London.

Bellotti, G., 2020. A modal decomposition method for the analysis of long waves amplification at coastal areas. Coast. Eng. 157.

Bellotti, G., Briganti, R., Beltrami, G., 2012a. The combined role of bay and shelf modes in tsunami amplification along the coast. J. Geophys. Res.-Oceans 117.

Bellotti, G., Briganti, R., Beltrami, G., Franco, L., 2012b. Modal analysis of semi-enclosed basins. Coast. Eng. 64, 16–25.

Bellotti, G., Romano, A., 2017. Wavenumber-frequency analysis of landslide-generated tsunamis at a Conical island. Part II: Eof and modal analysis. Coast. Eng. 128, 84–91.

Blondeaux, P., Seminara, G., Vittori, G., 1993a. Linear response of the gate system for protection of the venice lagoon. Note i: transverse free modes. Atti Accad. Naz. Lincei. Cl. Sci. Fis. Mat. Nat. Rend. Linc. Mat. Appl. 4, 291–298.

Blondeaux, P., Seminara, G., Vittori, G., 1993b. Linear response of the gate system for protection of the Venice lagoon. Note II: Excitation of transverse suhharmonic modes. Atti Accad. Naz. Lincei. Cl. Sci. Fis. Mat. Nat. Rend. Linc. Mat. Appl. 4, 299–305.

Carniello, L., Defina, A., Fagherazzi, S., D'Alpaos, L., 2005. A combined wind wave–tidal model for the Venice lagoon, Italy. J. Geophys. Res.: Earth Surf. 110.

Consorzio-Venezia-Nuova, 1988. Study on the Influence of the Inclination Angle and the Gate Shape on Gate Response. Technical Report, Delft Hydraulics, Technical Rep. Studio 2.2 . Magistrato alle Acque.

Consorzio-Venezia-Nuova, 2002a. Prove su Modello Fisico Della Bocca di Chioggia in Scala 1:60 Presso Il Centro Sperimentale di Voltabarozzo. Technical Report Technital B.05.73, Tests on a Physical Model of the Chioggia Inlet in 1:60 Scale at the Voltabarozzo Experimental Centre, (in Italian). Magistrato alle Acque.

Consorzio-Venezia-Nuova, 2002b. Realizzazione di Una Serie di Prove di Moto Ondoso sul Modello Fisico Della Bocca di Malamocco. Realization of a Series of Waves Tests on the Physical Model of the Malamocco Inlet. Technical Report Technital B.06.54, (in Italian). Magistrato alle Acque.

Consorzio-Venezia-Nuova, 2002c. Studio Sugli Effetti Scala Nelle Prove in Modello Fisico Delle Paratoie. Study on Scale Effects in Physical Model Tests of the Gates. Technical Report Technital B.06.53, (in Italian). Magistrato alle Acque.

Consorzio-Venezia-Nuova, 2003a. Realizzazione di Una Serie di Prove Sul Modello Fisico Della Bocca di Lido in Scala 1:64. Realization of a Series of Tests on the Physical Model of the Bocca Di Lido in 1:64 Scale. Technical Report Protecno B.06.63, (in Italian). Magistrato alle Acque.

Consorzio-Venezia-Nuova, 2003b. Studio Sulla Risonanza Sincrona Dei Modi Propri Della Schiera di Paratoie. Study on the Synchronous Resonance of the Natural Modes of the Gate Array. Technical Report, M.I.T. Dept. Civil Engineering, Technital, Protecno B.06.66. (in Italian). Magistrato alle Acque.

Consorzio-Venezia-Nuova, 2009. Bocca di Chioggia. Impianti Pneumatici. Chioggia Inlet. Pneumatic Facilities. Technical Report Technital MV100P, (in Italian). Magistrato alle Acque.

Defant, A., 1961. Physical oceanography.

Fagherazzi, S., Bortoluzzi, A., Dietrich, W.E., Adami, A., Lanzoni, S., Marani, M., Rinaldo, A., 1999. Tidal networks: 1. Automatic network extraction and preliminary scaling features from digital terrain maps. Water Resour. Res. 35, 3891–3904.

Gačić, M., Mosquera, I.M., Kovačević, V., Mazzoldi, A., Cardin, V., Arena, F., Gelsi, G., 2004. Temporal variations of water flow between the Venetian lagoon and the open sea. J. Mar. Syst. 51, 33–47.

Giupponi, C., Bidoia, M., Breil, M., Di Corato, L., Gain, A.K., Leoni, V., Fard, B.M., Pesenti, R., Umgiesser, G., 2024. Boon and burden: economic performance and future perspectives of the venice flood protection system. Reg. Environ. Change 24 (44).

Hersbach, H., Bell, B., Berrisford, P., Hirahara, S., Horányi, A., Muñoz-Sabater, J., Nicolas, J., Peubey, C., Radu, R., Schepers, D., et al., 2020. The era5 global reanalysis. Quart. J. R. Meteorol. Soc. 146 (730), 1999–2049.

Li, G., Mei, C.C., 2003a. Natural modes of mobile flood gates. Appl. Ocean Res. 25, 115–126.

Li, G., Mei, C.C., 2003b. Natural Modes of Mobile Gates for Venice Inlets. Computational Manual for a Barrier of Inclined Gates in a Channel. Technical Report, Technital, Protecno Report IV, M.I.T. Dept. Civil Engineering, Consorzio Venezia Nuova Magistrato alle Acque.

Liao, C.Y., Mei, C.C., 2000. Numerical solution for trapped modes around inclined venice gates. J. Waterw., Port Coast. Ocean Eng. 126, 236–244.

Lionello, P., Barriopedro, D., Ferrarin, C., Nicholls, R.J., Orlić, M., Raicich, F., Reale, M., Umgiesser, G., Vousdoukas, M., Zanchettin, D., 2021. Extreme floods of venice: characteristics, dynamics, past and future evolution. Nat. Hazards Earth Syst. Sci. 21, 2705–2731.

Međugorac, I., Orlić, M., Janeković, I., Pasarić, Z., Pasarić, M., 2018. Adriatic storm surges and related cross-basin sea-level slope. J. Mar. Syst. 181, 79–90.

Mei, C.C., Sammarco, P., Chan, E., Procaccini, C., 1994. Subharmonic resonance of proposed storm gates for Venice lagoon. Proc. R. Soc. Lond. Ser. A Math. Phys. Eng. Sci. 444, 257–265.

Mel, R.A., Coraci, E., Morucci, S., Crosato, F., Cornello, M., Casaioli, M., Mariani, S., Carniello, L., Papa, A., Bonometto, A., et al., 2023. Insights on the extreme storm surge event of the 22 november 2022 in the Venice lagoon. J. Mar. Sci. Eng. 11 (1750).

Orlić, M., Kuzmić, M., Pasarić, Z., 1994. Response of the adriatic sea to the bora and sirocco forcing. Contin. Shelf Res. 14, 91–116.

Panizzo, A., Sammarco, P., Bellotti, G., De Girolamo, P., 2006. Eof analysis of complex response of venice mobile gates. J. Waterw. Port Coast. Ocean Eng. 132, 172–179.

Pasquali, D., Bruno, M., Celli, D., Damiani, L., Di Risio, M., 2019. A simplified hindcast method for the estimation of extreme storm surge events in semi-enclosed basins. Appl. Ocean Res. 85, 45–52.

Sammarco, P., Tran, H.H., Gottlieb, O., Mei, C.C., 1997b. Subharmonic resonance of venice gates in waves. Part 2. Sinusoidally modulated incident waves. J. Fluid Mech. 349, 327–359.

Sammarco, P., Tran, H.H., Mei, C.C., 1997a. Subharmonic resonance of venice gates in waves. Part 1. Evolution equation and uniform incident waves. J. Fluid Mech. 349, 295–325.

Tosi, L., Teatini, P., Strozzi, T., 2013. Natural versus anthropogenic subsidence of Venice. Sci. Rep. 3 (1), 2710.

Trincardi, F., Barbanti, A., Bastianini, M., Benetazzo, A., Cavaleri, L., Chiggiato, J., Papa, A., Pomaro, A., Sclavo, M., Tosi, L., et al., 2016. The 1966 flooding of Venice: What time taught us for the future. Oceanography 29, 178–186.

Vittori, G., 1997. Free and forced oscillations of a gate system as proposed for the protection of Venice lagoon: The discrete and dissipative model. Coast. Eng. 31, 37–58.

Vittori, G., Blondeaux, P., Seminara, G., 1996. Waves of finite amplitude trapped by oscillating gates. Proc. R. Soc. Lond. Ser. A Math. Phys. Eng. Sci. 452, 791–811.